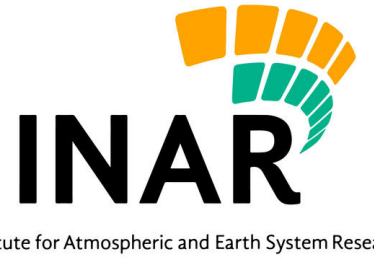

Master's thesis
Geophysics of the Hydrosphere
Master's Programme in Atmospheric Sciences

On the Use of Brunt-Väisälä Frequency as a Proxy for Surface Water pCO_2 in a Small Boreal Lake

Aleksi Arola

June 29, 2021

Supervisor: Docent Ivan Mammarella

Examiners: Professor Petteri Uotila
Docent Anne Ojala

UNIVERSITY OF HELSINKI
Faculty of Science
INAR - Institute for Atmospheric and Earth System Research

P.O. Box 64 (Gustaf Hällströmin katu 2)
FI-00014 University of Helsinki

HELSINGIN YLIOPISTO — HELSINGFORS UNIVERSITET — UNIVERSITY OF HELSINKI

Tiedekunta — Fakultet — Faculty	Koulutusohjelma — Utbildningsprogram — Education programme
Faculty of Science	Master's Programme in Atmospheric Sciences

Tekijä — Författare — Author
Aleksi Arola

Työn nimi — Arbetets titel — Title

On the Use of Brunt-Väisälä Frequency as a Proxy for Surface Water pCO_2 in a Small Boreal Lake

Opintosuunta — Studieinriktning — Study track
Geophysics of the Hydrosphere

Työn laji — Arbetets art — Level	Aika — Datum — Month and year	Sivumäärä — Sidoantal — Number of pages
Master's thesis	June 29, 2021	41 pages

Tiivistelmä — Referat — Abstract

Freshwater ecosystems are an important part of the carbon cycle. Boreal lakes are mostly supersaturated with CO_2 and act as sources for atmospheric CO_2. Dissolved CO_2 exhibits considerable temporal variation in boreal lakes. Estimates for CO_2 emissions from lakes are often based on surface water pCO_2 and modelled gas transfer velocities (k).

The aim of this study was to evaluate the use of a water column stratification parameter as proxy for surface water pCO_2 in lake Kuivajärvi.

Brunt-Väisälä frequency (N) was chosen as the measure of water column stratification due to simple calculation process and encouraging earlier results. The relationship between N and pCO_2 was evaluated during 8 consecutive May–October periods between 2013 and 2020. Optimal depth interval for N calculation was obtained by analysing temperature data from 16 different measurement depths. The relationship between N and surface pCO_2 was studied by regression analysis and effects of other environmental conditions were also considered.

Best results for the full study period were obtained via linear fit and N calculation depth interval spanning from 0.5 m to 12 m. However, considering only June–October periods resulted in improved correlation and the relationship between the variables more closely resembling exponential decay. There was also strong inter-annual variation in the relationship. The proxy often underestimated pCO_2 values during the spring peak, but provided better estimates in summer and autumn. Boundary layer method (BLM) was used with the proxy to estimate CO_2 flux, and the result was compared to fluxes from both BLM with measured pCO_2 and eddy covariance (EC) technique. Both BLM fluxes compared poorly with the EC flux, which was attributed to the parametrisation of k.

Avainsanat — Nyckelord — Keywords
Brunt-Väisälä frequency, surface water pCO_2, boreal lake, water column stratification, CO_2 fluxes

Säilytyspaikka — Förvaringsställe — Where deposited
Kumpula campus library

Muita tietoja — övriga uppgifter — Additional information

Contents

1 Introduction **1**

2 Theory **3**

2.1 Characteristics of boreal lakes 3

2.1.1 Overview 3

2.1.2 Seasonal stratification and mixing processes in boreal lakes . . 3

2.1.3 Surface energy balance 6

2.2 Freshwater ecosystems in the carbon cycle 7

2.2.1 Global importance of freshwater ecosystems 7

2.2.2 Carbon transport and transformation processes 8

2.2.3 CO_2 dynamics in boreal lakes 9

2.3 Gas exchange across the air-water interface 10

2.3.1 Basic theory 10

2.3.2 Gas fluxes based on boundary layer method 10

2.4 Gas fluxes based on eddy covariance technique 12

2.5 Brunt-Väisälä frequency 13

3 Materials and methods **14**

3.1 Site description 14

3.2 Data acquisition 15

3.3 Data analysis 16

3.3.1 Overview 16
3.3.2 Data for environmental conditions 16
3.3.3 Calculation of Brunt-Väisälä frequency 17
3.3.4 Flux of CO_2 18

4 Results and discussion **20**
4.1 Environmental conditions 20
4.1.1 Wind speed and direction 20
4.1.2 Air temperature and surface water temperature 21
4.1.3 Precipitation and snowmelt 22
4.1.4 Vertical thermal structure 23
4.1.5 Dissolved CO_2 25
4.2 Relationship between Brunt-Väisälä frequency and surface water pCO_2 27
4.2.1 N as a proxy for surface water pCO_2 27
4.2.2 Comparison to earlier studies promoting feasibility of Brunt-Väisälä frequency based proxy for dissolved CO_2 34
4.3 Comparison of CO_2 fluxes obtained via different methods 36
4.3.1 Comparison between CO_2 fluxes calculated from measurements and proxy 36
4.3.2 Comparison of eddy covariance and boundary layer method fluxes 37

5 Conclusions **39**

6 Acknowledgements **41**

Bibliography **42**

List of Figures

2.1 Schematic of simplified thermal stratification cycle and vertical layers in boreal lakes. Large arrows indicate mixing of entire water column during turnovers and smaller arrows denote relatively well mixed layers. T_1 and T_2 denote temperatures at upper and lower parts of the water column, respectively. 5

3.1 Map showing the bathymetry of lake Kuivajärvi and location of the measurement raft, which is marked with a red star. Bathymetry data for the map is from the Finnish Environment Institute and available at (https://www.avoindata.fi/data/fi/dataset/jarvien-ja-jokien-syvyysaineisto). 15

4.1 Wind rose based on 30-minute data from May–October 2013–2020 at Kuivajärvi and frequency histogram based on daily mean values of wind speed for the same time period. 20

4.2 Daily mean wind speeds recorded at lake Kuivajärvi in May–October 2013–2020. 21

4.3 Daily mean air temperature (red line) and surface water temperature (purple line) with the daily sums of precipitation (blue bars) for the May–October 2013–2020 period. 22

4.4 Evolution of snow water equivalent during the winters preceeding 2013–2020 open water periods. 23

4.5 Contour plot of daily mean temperatures from May–October 2013–2020. Black lines represent 2 °C intervals and white space denotes gaps in the data. 24

4.6 Daily mean pCO_2 at different depths during May–October 2013–2020. 26

4.7 Variation of daily mean lake surface pCO_2 during May–October 2013–2020. Black line represents mean of daily mean pCO_2 values measured at that time of year and the green shaded area outlines total variation from maximum to minimum. 27
4.8 Daily mean values of N calculated from 6 different depth intervals during the May–October 2013–2020 study period. 28
4.9 Scatter plots of N (20 cm – 500 cm) and both surface pCO_2 and CO_2 concentration during different years. 31
4.10 Best fits for daily mean N and both surface pCO_2 and CO_2 concentration during the complete May–October 2013–2020 study period. Data from May deviated noticeably from rest of the measurements and is highlighted in red color. 32
4.11 Scatter plots of monthly mean N (20 cm – 200 cm), and both pCO_2 and CO_2 concentration. Data from May is shown in red but is not part of the fit. 34
4.12 Daily mean CO_2 flux calculated from pCO_2 values predicted by the proxy (red) and from the measurements (blue). 37
4.13 Comparison between monthly mean CO_2 fluxes from BLM based on the measurements (blue) and proxy (red), and EC (yellow) during the May–October 2013–2020 study period. 38

List of Tables

4.1 Pearson correlation between daily means of N and surface pCO_2 (upper) and between N and surface CO_2 concentration (lower) for the May–October period during individual years and all study period. Upper N depth interval boundary of 50 cm resulted in slightly better results overall and is thus shown. 30

4.2 Pearson correlation between N and pCO_2 (upper), and N and CO_2 concentration (lower) for June–October period during individual years and all study period. Upper N depth interval boundary of 20 cm resulted in slightly better results for the June–October period and is thus shown. 33

1. Introduction

Freshwater ecosystems play an important role in the carbon cycle, and globally most lakes are supersatured with carbon dioxide (CO_2) which means that they act as sources rather than sinks for atmospheric CO_2 (Cole et al., 1994). These systems are not considered anymore to act as passive pipes, because in addition to transporting terrestrial carbon to the sea, they act as an active part of the carbon cycle by degassing considerable amounts of CO_2 to the atmosphere, and being the location for many transformation processes and sedimentary burial (Cole et al., 2007). The flux of carbon from inland waters to the atmosphere is assumed to even exceed the fraction transported all the way to the sea (Tranvik et al., 2009; Cole et al., 2007; Aufdenkampe et al., 2011).

The exchange of CO_2 between the lake environment and overlying atmosphere is commonly estimated via three different methods, which are eddy covariance technique (EC), flux chamber measurements (FC) and the boundary layer method (BLM). EC requires accurate high frequency measurements of wind components by a sonic anemometer and of CO_2 mixing ratio in the air by a gas sampler, while providing information on ecosystem scale and adequately covering even long periods of time, but at the same time being relatively expensive and requiring complex post-processing of data. FC measurements are done by measuring the rate of change of CO_2 concentration inside sealed floating chambers placed on the lake surface, and they provide better spatial, but worse temporal resolution than EC, while being simpler to deploy but manually laborous. Third option, BLM, is used to calculate the flux of CO_2 based on the difference between CO_2 concentrations at the water surface and air above, while the transfer rate is also controlled by the gas transfer velocity k. BLM is quite widely used, but prone to uncertainty in k and discrete spatio-temporal observations of pCO_2.

pCO_2 in freshwater ecosystems is affected by both physical and biological factors. Stratification, which acts to dampen turbulence and restricts vertical mixing, has been observed to have a major effect on lake surface pCO_2 (Huotari et al., 2009;

Åberg et al., 2010; Weyhenmeyer et al., 2012). The main objective of this thesis is to evaluate the use of a water column stability based proxy for surface water pCO_2 at lake Kuivajärvi. The proxy is used to estimate CO_2 flux between the lake and atmosphere by using BLM. The result obtained with the proxy will be evaluated against fluxes from both BLM with measured pCO_2 values and EC technique. This kind of proxy could be later used to improve CO_2 flux estimates from other lakes similar to Kuivajärvi. Earlier studies at lake Valkea-Kotinen, which is a humic boreal lake like Kuivajärvi, have shown that Brunt-Väisälä frequency (N) has a strong negative correlation with surface water CO_2 (Huotari et al., 2009, 2011). N can be used as a measure of water column stability and is simple to calculate from basic water column temperature measurements, making it a strong candidate for the proxy.

2. Theory

2.1 Characteristics of boreal lakes

2.1.1 Overview

Boreal lakes are typically relatively shallow, fresh and seasonally ice covered. While lakes can exhibit a number of different vertical circulation patterns, boreal lakes are in many cases dimictic, experiencing two full turnovers annually, one in the spring and one in the autumn. During the summer stratification all but the shallowest boreal lakes can be mostly divided into three parts: epilimnion at the top, thermocline in the middle and hypolimnion at the bottom. Dissolved humic substances give the water a yellow-brownish color while also reducing visibility and the euphotic depth. Lakes are present throughout most of the boreal zone and are even abundant in some areas, such as in the so called Finnish Lakeland. Boreal lakes are often located in depressions formed by processes during the last glacial period and surrounded by coniferous forest, from which the humic substances originate. Density of water and thus stratification of most boreal lakes is overwhelmingly governed by evolution of temperature, while salinity and pressure often play a negligible role.

2.1.2 Seasonal stratification and mixing processes in boreal lakes

Dimictic lakes experience two turnovers in a year with longer stratified periods between them. The spring turnover begins when the upper water column starts warming at the end of the stratified period in winter, during which colder water is on top of warmer due to the density maximum of freshwater occurring at $T = 4°C$. Turnover can already begin under the melting ice cover, as solar radiation is able to penetrate through snow-free ice and into the water column. Beginning from vicinity of the surface, the water column gradually warms and convective mixing advances

deeper. Finally the temperature profile will be close to uniform, and the water column is easily mixed by wind.

This continues until the summer stratification begins developing after the density maximum has been reached for the entire water column. Now further heating causes the water column to stabilize as water near the surface becomes lighter, leading to the stable summer stratification. Initially existing close to surface, the thermocline, sometimes termed metalimnion, is formed and divides the water column into a warmer and relatively well mixed surface layer, epilimnion, on top and cooler bottom layer, hypolimnion, under the thermocline. In addition to the seasonal thermocline, a diurnal thermocline can form inside the surface layer during the day due to intense heating, but it's considerably weaker than the seasonal thermocline and erodes during the cooling at night. During the summer depth and steepness of the seasonal thermocline is affected by interplay of periodical heating and cooling, and wind induced mixing.

The mixing surface layer is relatively uniform in terms of temperature and dissolved substance gradients, but exchange with deeper parts of the lake is minimal due to turbulent transport being supressed by the thermocline. The bottom layer isn't strongly stratified, but is often not as well mixed as the surface layer due to being insulated from sources of turbulence production. The separation from the surface also leads to both accumulation of substances produced in the hypolimnion and shortage of substances that are in demand.

In general the depth of the thermocline is also affected by lake size, as larger lakes are less sheltered from the wind, experiencing higher speeds and having longer fetches. Additionally the existence of thermocline allows for propagation of internal waves and prolonged strong winds can also lead to upwelling events.

Towards the end of summer lake begins to lose heat, resulting in gradual deepening of the seasonal thermocline and erosion of the stable summer stratification by convective mixing, which reaches deeper over time. The following period of water column mixing is termed the autumn turnover, and the vertical temperature profile is once again close to uniform, allowing vertical circulation of the water column. The duration of the overturn depends on prevailing weather conditions, but it generally lasts longer than the spring overturn. Ice formation is possible after the turnover ends when the water column has cooled down to the temperature of maximum density at $T = 4°C$, which allows the inverse winter stratification to form as further cooling of water no longer leads to convection, but instead acts to stabilize the water column. In calm and cold weather ice cover is quickly formed and the turnover ends,

but periods of strong wind and recurring above freezing temperatures can extend the turnover period, which results in colder overall water column in winter.

The newly formed ice cover acts as an insulator, hindering heat, mass and momentum exchange between the lake and overlying atmosphere, while also accumulating snow cover, resulting in increased albedo and thus reduced solar radiation under the ice. During the inverse stratification in winter, which is weaker than the summer stratification, the coldest and now the lightest water is found directly under the ice cover at the surface and warmest water near the bottom of the lake, which can possibly be heated by the sediment heat flux to the temperature of density maximum. Even though the stratification in winter isn't nearly as strong as in the summer, effective mixing of the water column by wind acting on surface is prevented due to the protecting ice cover. Most important parts of the stratification cycle and the lake vertical layers are illustrated in Fig 2.1.

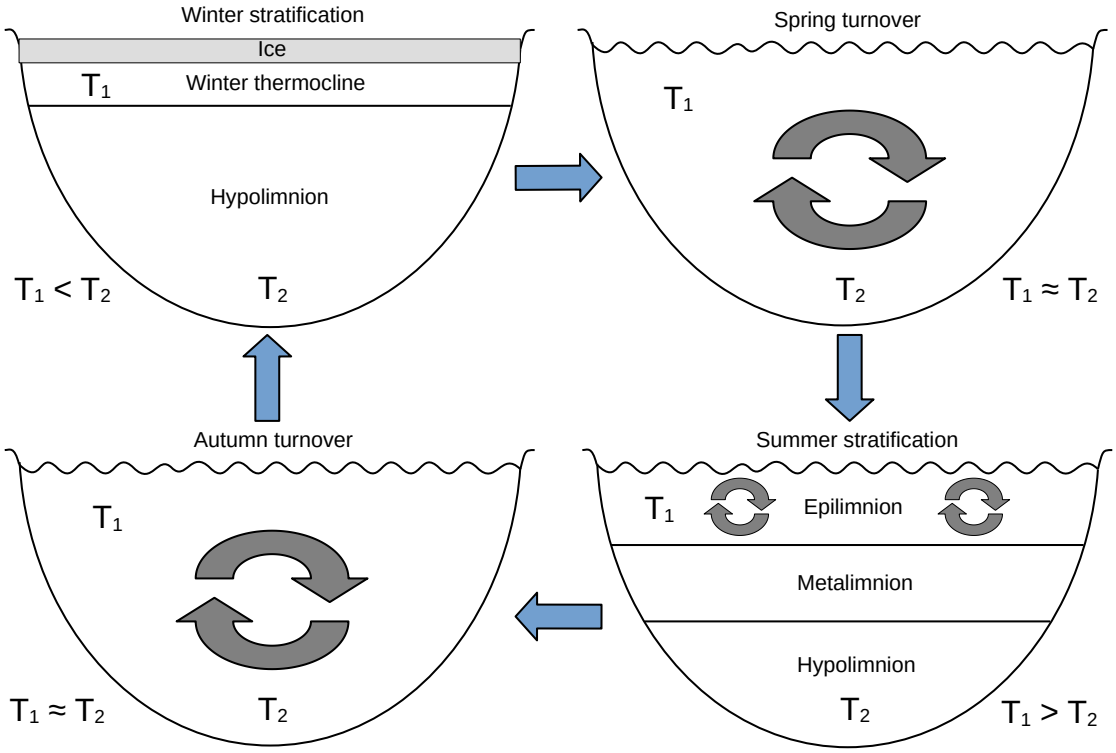

Figure 2.1: Schematic of simplified thermal stratification cycle and vertical layers in boreal lakes. Large arrows indicate mixing of entire water column during turnovers and smaller arrows denote relatively well mixed layers. T_1 and T_2 denote temperatures at upper and lower parts of the water column, respectively.

2.1.3 Surface energy balance

Exchange of heat occurring most importantly at the lake surface leads to the observed annual stratification cycle, which in turn controls many processes in boreal lakes. The heat fluxes are an essential part of lake dynamics due to temperature dependent water density changes playing an important role in water column stability related phenomena. The water colum heat storage change flux Q_{TOT} can be expressed as a sum of constituent fluxes.

$$Q_{TOT} = Q_{SW} + Q_{LW} + Q_{LH} + Q_{SH} + \sum Q_{other} \tag{2.1}$$

Heat fluxes in and out of the lake consist most importantly of radiative heat fluxes in the form of net shortwave radiation, Q_{SW}, and net longwave radiation, Q_{LW}, and turbulent heat fluxes consisting of latent heat flux, Q_{LH}, and the sensible heat flux, Q_{SH}. The water body also experiences heat fluxes from precipitation at the surface (generally small), heat flux from sediments (affecting water column in the vicinity of bottom, generally small) and heat flux through inflow from rivers, streams and groundwater and due to outflow, which are all denoted with $\sum Q_{other}$.

Q_{SW} is the total incoming solar radiation at the surface reduced by the fraction that is reflected back due to albedo and unlike the other constituents, it penetrates through surface into the water column according to Beer's law, also causing heating away from the surface. This penetration is in turn affected by dissolved and particulate substances in the water column. The diurnal average of Q_{TOT} is positive during the spring and summer, while being negative during the autumn and winter. Despite being positive on average during the warm seasons cooling happens during the night in absence of incoming shortwave radiation. Q_{SW} is always positive, resulting in net gain of heat for the lake, but varies greatly both diurnally and seasonally while also being affected by factors such as latitude and temporarily cloudiness.

Q_{LW} consists of heat loss due to emission of longwave radiation by the surface and gain of heat from incoming longwave radiation, emitted by the atmosphere and absorbed at the water surface. The emission of radiation is described by the Stefan-Boltzmann law, increasing exponentially with temperature, while cloud cover also affects the atmospheric emissivity. Q_{LW} always results in net loss of heat for the water surface due to higher emissivity if compared to the atmosphere.

The turbulent heat fluxes Q_{LH} and Q_{SH} consist respectively of heat losses and gains from phase transition occurring at the air-water interface, leading to a net loss of heat for the water surface due to evaporation and the direct sensible heat exchange between the water surface and air over it, direction of which depends on

the relative temperatures. Both of these fluxes are greatly affected by prevailing wind conditions, while latent heat flux is also affected by humidity of air relative to saturation and sensible heat flux by the magnitude of the temperature difference.

2.2 Freshwater ecosystems in the carbon cycle

2.2.1 Global importance of freshwater ecosystems

Despite covering only a small fraction of the land area, freshwater systems consisting of lakes, reservoirs, rivers and streams are an important part of the global carbon cycle. They not only transport carbon from land to sea as was earlier presumed, but they release considerable amount of carbon most importantly in the form of CO_2, but also methane, CH_4, into the atmosphere. While this evasion occurs at the water surface, burial of carbon in sediments constitutes a sink for terrestrial carbon, while additional transformation processes occur during the journey in the water column. Outgassing and burial of carbon in freshwater systems are both of the same magnitude as the amount of carbon transported all the way to the sea, however there is some variation in the estimates.

Estimates for carbon emissions mainly in the form of CO_2 from freshwater systems as a whole vary between 2.1 Pg C yr^{-1} (Raymond et al., 2013) and 0.75 Pg C yr^{-1} (Cole et al., 2007), while Tranvik et al. (2009) gives a number of 1.4 Pg C yr^{-1} and Battin et al. (2009) 1.2 Pg C yr^{-1}. However, the estimate by Cole et al. (2007) is stated to be conservative. The part of lakes and reservoirs of these numbers is 0.32 Pg C yr^{-1} according to Raymond et al. (2013), while Tranvik et al. (2009) gives 0.53 Pg C yr^{-1} as the upper end when combining results of earlier studies. According to Cole et al. (2007) CO_2 flux from lakes to atmosphere is 0.11 Pg C yr^{-1} and from reservoirs 0.28 Pg C yr^{-1}. Aufdenkampe et al. (2011) gives the global value of 0.64 Pg C yr^{-1} for lakes and reservoirs combined, 0.56 Pg C yr^{-1} for rivers and streams and 2.08 Pg C yr^{-1} for wetlands, which are closely linked to freshwater systems in general, but not considered in other mentioned studies due to their too different characteristics. In the much earlier paper by Cole et al. (1994) emissions from lakes alone were estimated to be 0.14 Pg C yr^{-1}.

Burial rates of carbon in the freshwater systems are assumed to be smaller, but of the same magnitude as the fluxes to atmosphere and the estimates vary between 0.23 Pg C yr^{-1} (Cole et al., 2007) and 0.6 Pg C yr^{-1} (Battin et al., 2009; Tranvik et al., 2009). The total inland flux of carbon to the freshwater systems is estimated

to be from 1.9 Pg C yr^{-1} (Cole et al., 2007) to 2.7 Pg C yr^{-1} (Battin et al., 2009) and 2.9 Pg C yr^{-1} (Tranvik et al., 2009) and the part transported to the sea 0.9 Pg C yr^{-1} by all of the three earlier sources.

2.2.2 Carbon transport and transformation processes

Important pathway for carbon to enter lacustrine systems is through groundwater and stream flow in the catchment. The water system gains both inorganic and organic carbon through these flows, and the amounts are dependent on the productivity of the surrounding area and flow path, while the origin of both organic and inorganic carbon transported this way is the terrestrial primary production. Other possible pathway for carbon into the system is through gas transfer at the air-water interface, but this isn't the case for most inland waters, as generally only eutrophic systems have high enough demand for CO_2 to be undersatured in relation to the atmosphere. After entering the water system some of the carbon undergoes transformation processes, while some is transported further via outflow. Majority of organic carbon entering aqueous inland systems is in dissolved form, while much smaller part is in form of detrital soil and plant material. Eventually after possibly going through multiple transformation processes the carbon is either outgassed mainly in the form of CO_2 (in the case of supersaturation), sedimented to the bottom or transported all the way through the system to the sea (Cole and Prairie, 2010a).

Carbon residing in the water column can be divided to inorganic and organic carbon, of which inorganic carbon exists in the form of dissolved inorganic carbon (DIC) and organic carbon in the forms of dissolved organic carbon (DOC) and particulate organic carbon (POC). However, the largest carbon pools in freshwater systems are found in the sediments, but they're not operating at the same time scale as carbon suspended in the water column. Transformation of carbon from inorganic to organic occurs through photosyntesis, and from organic to inorganic through respiration processes (Cole and Prairie, 2010a).

DIC consists of bicarbonate ions (HCO_3), carbonate ions (CO_3) and most importantly in terms of this thesis carbon dioxide, CO_2, small part of which exists in it's hydrated form, H_2CO_3. The relative concentrations of HCO_3, CO_3 and CO_2 are linked to pH value in the water system, low values indicating high relative amount of HCO_3 , medium values high CO_2 and high values high CO_3. Even though most of DIC isn't necessarily in the form of CO_2, it's the most dynamic and generally considered the most important constituent. CO_2 in water systems mainly

originates from different respiration processes, which cause majority of lakes to be supersaturated with CO_2. (Cole and Prairie, 2010b).

In most lakes the CO_2 supersaturation with respect to atmosphere can be explained by the uneven balance between respiration processes and primary production through photosynthesis. Respiration means the total biological oxidation of CO_2 by organisms of different types and sizes ranging from microbes to plants and fauna. Photosynthesis is the process responsible for biological consumption of dissolved CO_2 to produce organic matter. CO_2 can also be produced through means of abiotic oxidation of organic matter by UV-radiation, but it's generally not as important as the biological production. Inputs of CO_2 also happen through inflow when respiration of originally terrestrial biomass has occurred before arrival in the main water system. Chemical and physical factors can also play a role in CO_2 saturation, as changes in pH value result in changes to balance between constituents of DIC, while stratification leads to uneven distribution of dissolved CO_2 in the water column (Cole and Prairie, 2010b).

2.2.3 CO_2 dynamics in boreal lakes

The periods of mixing and stratification in boreal lakes are important for the exchange of CO_2 with the atmosphere. During the stratified period in summer, accumulation of dissolved CO_2 is possible in the hypolimnion, which is effectively prevented from exchanging substances with the surface layer due to the thermocline (Miettinen et al., 2015). In the surface layer dissolved CO_2 is consumed by photosynthesis and exchanged with the overlying atmosphere, but resupply from the deeper parts of the lake is prevented. Photosynthetic activity also results in diurnal variation of CO_2 in the surface layer during summer (Huotari et al., 2009).

Separation from the surface layer can also lead to levels of dissolved oxygen (O_2) dropping near the lake bottom during stratified period, as O_2 is consumed in respiration processes. During lake turnovers the accumulated CO_2 and other substances are vented, increasing their respective concentrations in the water column and at the air-water interface, which leads to an increase in fluxes to the atmosphere as well (Huotari et al., 2009; Miettinen et al., 2015). Lake turnovers also replenish the dissolved oxygen levels in lower part of the water column.

Accumulation of CO_2 can also happen during the winter under ice, as exchange with the atmosphere is prevented and photosynthesis hindered by the ice cover, while respiration continues (Karlsson et al., 2013).

Lakes in Finland, and boreal lakes overall, tend to be constantly supersaturated

with CO_2, which results in an upward flux to the atmopshere. They receive inputs of both organic and inorganic carbon from the surrounding area through inflow. Especially sediment respiration plays an important role in the CO_2 supersaturation of Finnish lakes and the accumulation of CO_2 occurring in the lower part of the water column during stratified period in summer. Rates of CO_2 evasion are higher from small and shallow lakes if compared to larger and deeper ones, and the CO_2 supersaturation is linked to undersaturation of O_2. Boreal lakes play an important part in the carbon cycle by transferring originally terrestrially fixed carbon back into the atmosphere (Kortelainen et al., 2006).

2.3 Gas exchange across the air-water interface

2.3.1 Basic theory

Gas transfer across the air-water interface is a diffusive process, which occurs in a very thin sub-layer at the surface, where molecular diffusion is the dominant transport process. The diffusive flux is written according to Fick's law

$$F = -D\frac{\partial C}{\partial z} \tag{2.2}$$

where D is the coefficient for molecular diffusion and $\frac{\partial C}{\partial z}$ represents the gas concentration gradient. Turbulence is responsible for transporting gas to the vicinity of the surface boundary, but is dampened due to viscous forces close to the boundary and the transport in the sub-layer near the surface is done by molecular diffusion. Stronger turbulence leads to thinner diffusive sub-layer at the surface, strenghtening the gas concentration gradient while the molecular diffusion coefficient is in turn affected by temperature and salinity (Bade, 2010).

2.3.2 Gas fluxes based on boundary layer method

The value of the concentration gradient related to Fick's law is difficult to quantify due to the extremely small thicknesses of the diffusive sub-layers at air-water interfaces. It can be reconstructed to consists of a gas transfer velocity multiplied by the gas concentration difference across the interface. In practical use of the boundary layer method, BLM, the gas flux F (for example in units of mol m^{-2} s^{-1}) is obtained from

$$F = k(C_{sur} - C_{eq}) = kK_h(p_{water} - p_{air}) \tag{2.3}$$

where k is the gas transfer velocity (m s^{-1}), C_{sur} the gas concentration (mol m^{-3}) at the water surface and C_{eq} the concentration that the gas at the water surface would have if it was in equilibrium with the overlying atmosphere (MacIntyre et al., 1995). As a further development the gas concentrations can also be expressed through partial gas pressures in the surface water and air above (p_{water} and p_{air}) and solubility coefficient K_h.

Conceptually k can be thought as the depth of water which is brought to equilibrium with the atmosphere in terms of chosen gas concentration in a given unit of time. Additionally k can be seen as D/z, where z is the thickness of the diffusive sublayer (Bade, 2010). Empirical models for k are traditionally based on wind speed, which seems to be the controlling factor for water side turbulence enhancing the air-water gas exchange when the wind speed is high. These models are generally called as boundary layer models, and a widely used wind speed based formulation, which was also chosen for this thesis, is k_{CC} (Cole and Caraco, 1998)

$$k_{CC} = (2.07 + 2.15U_{10}^{1.7})(\frac{Sc}{600})^{-n} \tag{2.4}$$

where U_{10} is the wind speed (m s^{-1}) at 10 m height and Sc the Schmidt number, formulated as ν/D, where ν is the kinematic viscosity. Here, Sc links kinematic viscosity of water to molecular diffusivity of gasses, describing the relative thickness of the hydrodynamic boundary layer to the diffusive sub-layer, where mass transfer of gas occurs. It's an important factor regarding gas transfer at the air-water interface and can also be used to relate gas transfer velocities for different gasses and temperatures to each other. Gas transfer velocities are often normalized to $Sc = 600$, which corresponds to CO_2 in freshwater at temperature of 20 C°. The exponent n in Eq 2.4 is chosen for local conditions and often varies between $\frac{1}{2}$ and $\frac{2}{3}$. Also more complicated formulations for k exist, such as surface renewal models incorporating the buoyancy flux, but for simplicity they're not used in this thesis. While k based gas transfer models can be tuned to account for many processes concerning gas exchange between the lake environment and atmosphere, certain phenomena such as emissions due to ebullition or through roots of aquatic plants cannot be accounted for in this framework (Bade, 2010).

The corresponding gas concentrations for CO_2 flux calculation via Eq. 2.3 can be obtained via Henry's law. Surface water pCO_2 is typically obtained from measurements done either in the field or lab by equilibrating a large sample of water with a small volume of air, from which pCO_2 is then measured. The pCO_2 in air, used to obtain the equilibrium concentration in Eq. 2.3, can be either measured locally

or taken as a constant based on time and location. Additionally it's possible to obtain CO_2 concentration through calculation from a combination of other available measurements (Temperature, DIC, alkalinity, pH) (Cole and Prairie, 2010b).

2.4 Gas fluxes based on eddy covariance technique

In this thesis the CO_2 fluxes obtained with BLM are compared to the flux obtained with the eddy covariance (EC) method, and thus a short introduction to the topic is given. The EC method is a direct micrometeorological measurement technique that can be used to obtain the turbulent fluxes of momentum, heat and gases. It can be applied to a range of different locations ranging from forests and fields all the way to sea and lakes, but the site and prevalent meteorological conditions must still meet certain criteria for the theoretical assumptions of EC to be valid. While requiring relatively expensive setup and complex post-processing, it offers data on ecosystem level with good temporal coverage and spatiotemporal resolution, capable of capturing diurnal, seasonal and special event related variations in the fluxes. Measurements are done by a sonic anemometer for the three wind components and temperature, and by a gas analyzer for the target gas, both instruments sampling at a high frequency. These devices are mounted on towers of varying height and type designed to fit the measurement site and the data is logged on a computer (Munger et al., 2012; Rebmann et al., 2012). In addition to these instrumental requirements, the obtained data needs to be quality controlled to match numerous criteria, and depending on the purpose, can be filled for gaps before interpreting (Foken et al., 2012; Rebmann et al., 2012).

EC fluxes are obtained from covariance between the vertical wind speed component and of other desired variable, such as longitudinal wind speed components for momentum or mixing ratio of CO_2 for the flux of CO_2.

Distinct features of lakes in terms of EC measurements are generally smaller fluxes of CO_2 and longer flux footprints if compared to vegetated land areas. In some cases defining the outlines of the lake can also be problematic, and special consideration may be required depending on the type of the littoral zone. The atmospheric boundary layer over a lake also differs from that over land due to the lake's ability to effectively store heat. This heat storing capacity affects stability above the lake surface on both diurnal and seasonal scale. Advection of air from the surrounding landscape to the lake can also affect measurements during stable conditions, and measurement instruments should be located on a platform in the

lake instead of the shores. It should also be noted that without additional in lake measurements it might be difficult to intepret some of the results of EC measurements, as a change in fluxes might not necessarily depend on turbulence conditions, but lake side processes instead (Vesala et al., 2012).

2.5 Brunt-Väisälä frequency

Brunt-Väisälä frequency (N), also called buoyancy frequency, can be used as a measure of stability for a fluid column and is written as

$$N = \sqrt{-\frac{g}{\rho}\frac{\partial \rho}{\partial z}} \tag{2.5}$$

where g is the gravitational acceleration, ρ density and z depth. N describes how a fluid parcel would oscillate after being vertically displaced. In the case of stable stratification N is positive and larger positive values indicate stronger stratification, leading to higher frequency of oscillation and therefore results in lower oscillatory period, while weaker stratification results in longer oscillatory period. In a case with neutral stratification N has the value of zero, and the displacement doesn't lead to any oscillatory motion. Finally in a case of unstable stratification N has complex values and there is no oscillation, as the parcel doesn't return to its original position, but is instead accelerated away. Unstable conditions tend to thus break and if observed they indicate active overturning process and convective mixing.

3. Materials and methods

3.1 Site description

The study site was lake Kuivajärvi (61°50′ N, 24°17′ E), which is a small mesotrophic and dimictic humic boreal lake located in Juupajoki, Hyytiälä in southern Finland. The location is also home to Hyytiälä Forestry Field Station and the measurements at the lake are part of SMEAR II (Station for Measuring Ecosystem Atmosphere Relations, Hari and Kulmala (2005)). Lake Kuivajärvi is located in the upper part of Kokemäenjoki drainage basin, which drains to the Sea of Bothnia in the Baltic Sea. The lake has an elongated shape, being around 2.6 km long in the northwest-southeast direction with maximum width of around 500 m. The lake consist of two main basins, deeper of which has a maximum depth of 13.2 m and also hosts the measurement raft used for collecting the data used in this thesis. Lake bathymetry and location of the raft are shown in Fig. 3.1. Surface area is around 0.62 km^2 and the mean depth 6.3 m. Catchment area is around 9.4 km^2 and the lake is surrounded mostly by managed coniferous forest, but some of the catchment area is also covered by peatland and to much lesser extent agricultural land. Variation of terrain height in the catchment area is up to 40 m, but most of it is flat. Haplic Podzol is the primary soil type in the area (Miettinen et al., 2015). Water clarity is low mainly due to high DOC, which is 11.8–14.1 mg l^{-1}, while total nitrogen and phosphorus concentrations are 370–500 µg l^{-1}, and 14–21 µg l^{-1}, respectively (Miettinen et al., 2015). The Secchi depth of Kuivajärvi is around 1.2–1.5 m (Heiskanen et al., 2015). Long-term mean temperature and annual precipitation were 3.5 °C and 711 mm during 1981–2010 (Pirinen, 2012), while the long-term mean duration of lake ice cover in the area of Kuivajärvi is between 150–170 days and maximum thickness between 50–60 cm according to statistics between 1961–2000 (Korhonen, 2005).

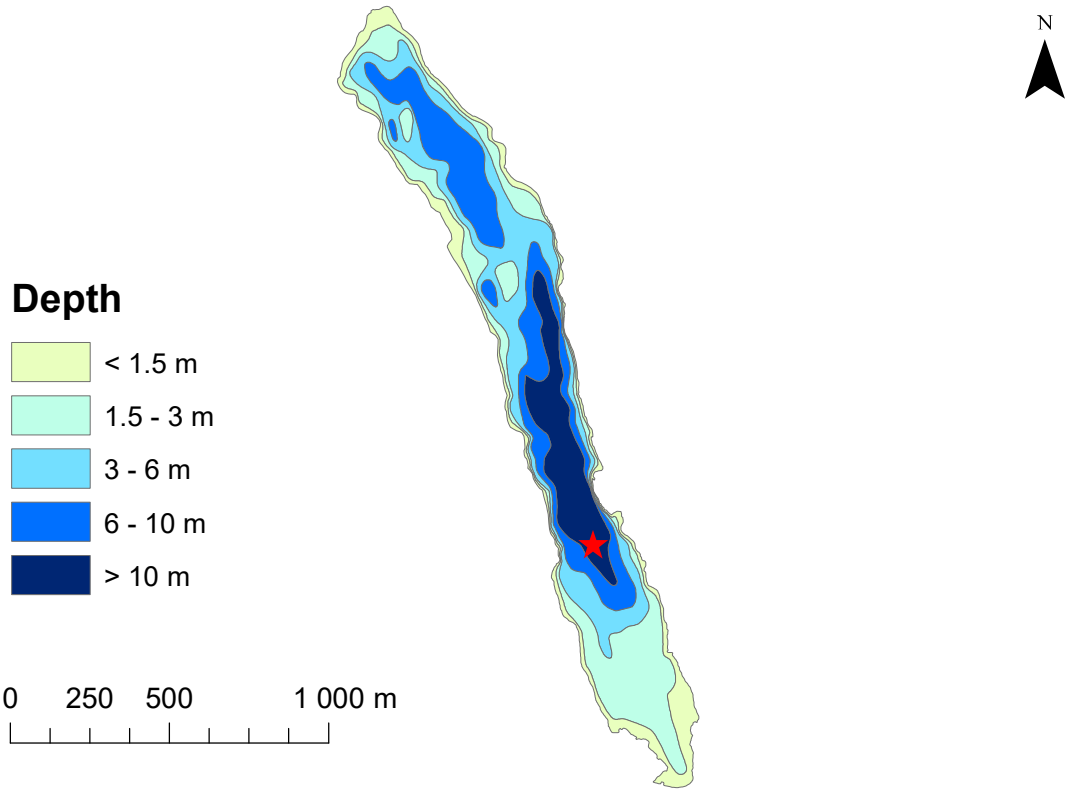

Figure 3.1: Map showing the bathymetry of lake Kuivajärvi and location of the measurement raft, which is marked with a red star. Bathymetry data for the map is from the Finnish Environment Institute and available at (https://www.avoindata.fi/data/fi/dataset/jarvien-ja-jokien-syvyysaineisto).

3.2 Data acquisition

Measurement data from Kuivajärvi is openly available and was downloaded from AVAA SmartSMEAR service (https://smear.avaa.csc.fi/download) with 30 minute temporal resolution. The continuous automatic measurements done at the moored raft in the southern basin of Lake Kuivajärvi include both underwater and above surface measurements and provide data with good temporal coverage. The underwater measurements include temperature monitoring at 0.2, 0.5, 1.0, 1.5, 2.0, 2.5, 3.0, 3.5, 4.0, 4.5, 5.0, 6.0, 7.0, 8.0, 10.0 and 12.0 m depths by a thermistor chain consisting initially of Pt100 sensors and after 11/2019 RBR-thermistors, and CO_2 measurements from 0.2, 1.5, 2.5 and 7.0 m depths by Vaisala CARBOCAP GMP343 CO_2 analyzers. Structure of the aquatic CO_2 measurement system is similar to the one used by Hari et al. (2008), and is explained in detail in that paper. Photosynthetically active radiation (PAR) is also measured by Li-Cor Li-192 underwater quantum sensors at four different depths.

Measurements above the lake surface are most importantly done by an EC setup at the height of 1.5 m. Fluxes measured this way include sensible and latent heat, momentum, CO_2 and H_2O. Gas concentrations are measured with LI-COR LI-7200 gas analyzer, while wind components and temperature are measured with Metek USA-1 anemometer/thermometer. These measurements also provide data for the calculation of additional parameters such as mean wind speed and direction, Monin-Obukhov length and friction velocity.

Air temperature and relative humidity are also measured at 2 m height by Pt100 sensor and Rotronic MP102H, respectively. Measurements of radiation include global shortwave radiation, reflected shortwave radiation and both incoming and outgoing far-infrared radiation, measured by Kipp & Zonen CNR1 radiometer.

Additionally air temperature and precipitation data for Juupajoki was obtained from the Finnish Meteorological Institute (https://www.ilmatieteenlaitos.fi/avoin-data) with daily and monthly temporal resolutions. Snow water equivalent data with temporal resolution of two weeks was obtained from the Finnish Environment Institute through the Hertta service (https://www.syke.fi/fi-FI/Avoin_tieto/Ymparistotietojarjestelmat).

3.3 Data analysis

3.3.1 Overview

Relationship between N and pCO_2 was analyzed based on data collected during 8 consecutive May–October periods in 2013–2020. This yearly span of 6 months was chosen to avoid the ice cover but still include at least most of the turnover periods in spring and autumn. The fluxes of CO_2 were also obtained for the same time period. For environmental conditions focus was on the May–October period, but as the conditions during the open water season are also affected by previous events, analysis was extended to cover longer periods when appropriate.

3.3.2 Data for environmental conditions

Most of the data obtained from the raft at Kuivajärvi with 30 minute temporal resolution was averaged to daily mean values for the analysis of environmental conditions.

Wind conditions were analysed both at the original 30 minute resolution and at daily mean level. Evolution of air temperature was observed through two types

of measurements made at the raft in lake Kuivajärvi in addition to the open data made available by Finnish Meteorological Institute. All three of the measurements were mostly in very good agreement with each other and the Finnish Meteorological Institute data was chosen for representation due to being continuous throughout the study period, whereas the data from the raft had few gaps. Precipitation data obtained from the Finnish Meteorological Institute was analysed as both daily and monthly sums and compared to statistics. Evolution of the surface water temperature was observed during the study period through water temperature measurements made at 20 cm depth at the raft in the lake.

Snow water equivalent (SWE) data for the winters and springs preceeding each of the analysed open water periods were obtained from the Finnish Environment Institude. SWE data is available for certain locations with a temporal resolution of two weeks, and the values are based on snow line measurements and model results, dependent on location and time. While there are no values given for Kuivajärvi, linear interpolation to obtain an estimate was made between the two nearest available locations, Mänttä-Vilppula, Vilppula (62.01427 N, 24.50472 E) and Näsijärvi-Tammerkoski, Tampere (61.4963 N, 23.76393 E), approximately 22 km and 48 km distance away from Kuivajärvi, respectively. While the interpolated values won't provide exactly correct values for Kuivajärvi, they're certainly good enough to make comparisons between the prevailing conditions during the springs of different years.

3.3.3 Calculation of Brunt-Väisälä frequency

Temperature data from all available measurement depths (0.2, 0.5, 1.0, 1.5, 2.0, 2.5, 3.0, 3.5, 4.0, 4.5, 5.0, 6.0, 7.0, 8.0, 10.0 and 12.0 m) was used in the analysis. Values for N were first calculated from the original data consisting of 30 minute arithmetic means, but both daily and monthly mean values of N were obtained by further averaging of the initially calculated values. Daily averaging was done to reduce random error and ignore possible effects related to the diurnal cycle, while still maintaining sufficient temporal resolution to notice effects of relatively short-term variations in the water column stability. Calculation of N was made according to Eq. 3.1

$$N = \sqrt{-\frac{g}{\rho}\frac{\Delta\rho}{\Delta z}} = \sqrt{-\frac{g}{\rho}\frac{\rho_1 - \rho_2}{z_2 - z_1}} \tag{3.1}$$

where z_1 and z_2 are the upper and lower bound of the depth interval, respec-

tively. ρ_1 is the water density at z_1 and ρ_2 at z_2. It should be noted that for Eq. 3.1 the depths z_1 and z_2 are taken as positive towards the bottom of the lake. gravitational acceleration $g = 9.81$ m s^{-1} and ρ was taken as constant 1000 kg m^3 .

Upper boundaries for the depth intervals used in N calculations were 20 cm and 50 cm. Time series of N were calculated for each possible depth interval (20 cm to 50 cm, 20 cm to 100 cm etc.), resulting in 15 different intervals for $z_1 = 20$ cm and 14 for $z_1 = 50$ cm.

Values of ρ_1 and ρ_2 for Eq. 3.1 were obtained from Eq. 3.2, which is from Leppäranta et al. (2017) (p. 48).

$$\rho(T, 0, p_0) = 999.842594 + 6.793952 \cdot 10^{-2}T - 9.095290 \cdot 10^{-3}T^2 + 1.001685 \cdot 10^{-4}T^3 - 1.120083 \cdot 10^{-6}T^4 + 6.536332 \cdot 10^{-9}T^5 \quad (3.2)$$

T is temperature in °C. Instead of the full equation of state, a formula considering only temperature is appropriate for the study site. Kuivajärvi is a shallow freshwater lake and the effects of salinity and pressure on density are insignificant if compared to the effect of temperature.

The accuracy of Pt100 sensors used in the thermistor chain represented an issue especially when stratification conditions were close to neutral. Lacking accuracy might result in the stratification erroneously appearing unstable or in turn too stable, depending on the direction and magnitude of the measurement errors. The issue posed by measurement accuracy was somewhat remedied by transforming complex values for N (physically intrepreted as unstable stratification) to zero. Leaving the complex values out of the analysis results in small artificial increase in initial goodness of fit for the proxy equation, which doesn't in turn translate into actually better predictions for the values of surface pCO_2. However the Pt100 sensors were changed to RBR-thermistors in November of 2019, which presumably have better accuracy. The inaccuracy of the measurement instruments also resulted in inability to produce a vertical stability profile of the water column.

3.3.4 Flux of CO_2

Boundary layer method

The flux of CO_2 was calculated according to Eq. 2.3 for both pCO_2 values obtained from the measurements and pCO_2 values predicted by the proxy. Atmospheric pCO_2 was taken as constant 400 μatm. Sensor output of aquatic CO_2 measurements at

Kuivajärvi is in units of ppm, which corresponds to mixing ratio, X_{CO_2}. Pressure inside the measurement system is close to atmospheric value. The values of pCO_2, X_{CO_2} and C_{CO_2} are linked by Eq. 3.3

$$C_{CO_2} = X_{CO_2} p_a K_h = pCO_2 K_h, \tag{3.3}$$

where p_a is the atmospheric pressure. Henry's solubility K_h (mol l^{-1} atm^{-1}) was calculated from the temperature measurements at 20 cm depth according to Eq. 3.4 (Wanninkhof, 2014)

$$\ln K_h = A_1 + A_2(\frac{100}{T}) + A_3 \ln(\frac{T}{100}), \tag{3.4}$$

where T is temperature in Kelvins. Constants in the equation are as follows: $A_1 = -58.0931$, $A_2 = -90.5069$, $A_3 = 22.2940$.

Gas transfer velocity used with Eq. 2.3 was k_{CC} (Cole and Caraco, 1998), calculated according to Eq. 2.4. $n = \frac{1}{2}$ was chosen as the exponent of Sc for scaling of k to local conditions at Kuivajärvi in accordance with (Erkkilä et al., 2018).

Local wind measurements were converted to 10 m values for calculation of k_{CC} (Eq. 2.4) according to the logarithmic wind profile via Eq. 3.5 (Bade, 2010)

$$U_{10} = U_x[1 + \frac{C_d^{0.5}}{\kappa}\ln(\frac{10}{x})], \tag{3.5}$$

where U_x is the measured wind speed and x the measurement height in meters, in this case $x = 1.5$. $C_d = 1.3 \times 10^{-3}$ is the drag coefficient at 10 m height and $\kappa = 0.4$ is the Von Karman constant. Strictly speaking Eq. 3.5 is valid only in neutral stability conditions, but it's sufficient for this purpose.

In the case of freshwater Sc is a function of temperature and was obtained from Eq. 3.6, which is based on a polynomial fit from Wanninkhof (2014), made according to results of Jähne et al. (1987):

$$Sc = 1923.6 - 125.06T + 4.3773T^2 - 0.085681T^3 + 0.00070283T^4, \tag{3.6}$$

where T is temperature in °C.

Eddy covariance data

Eddy covariance data was obtained in already postprocessed and quality flagged form from (https://smear.avaa.csc.fi/download), and only averaged to monthly level for the comparison of CO_2 fluxes. Only quality flag 0 (very good) was used.

4. Results and discussion

4.1 Environmental conditions

4.1.1 Wind speed and direction

According to the distribution of wind speed and direction, wind was predominantly channeled along the oblong shape of lake Kuivajärvi either in approximately northwesterly or southeasterly direction while the highest wind speeds were also recorded in these directions (Fig. 4.1). The maximum 30 min value was 10.44 m s^{-1} and the maximum daily mean wind speed 7.68 m s^{-1}, both recorded on 17.9.2020, while in turn the lowest daily mean value was 0.45 m s^{-1}. The mean wind speed for all analysed period was 1.99 m s^{-1} and median 1.61 m s^{-1}.

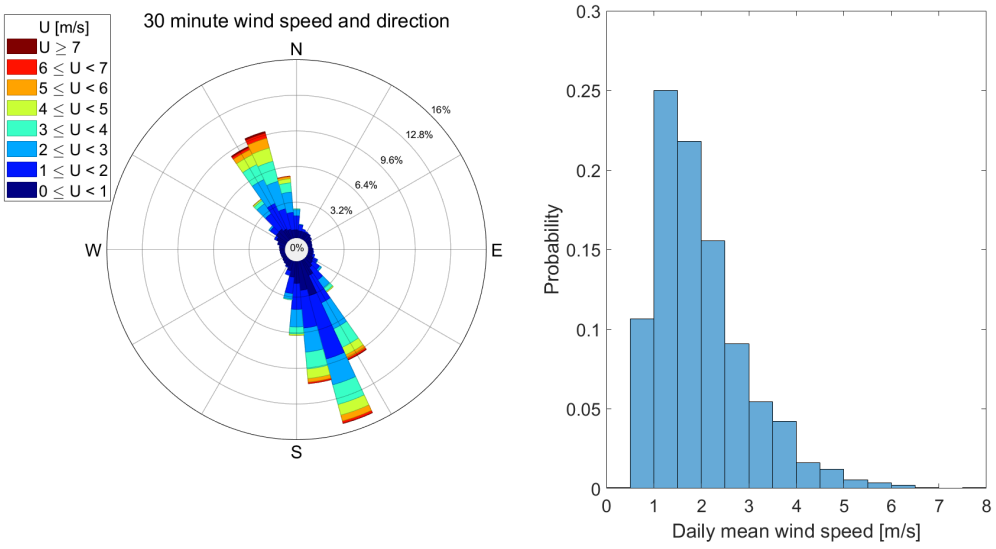

Figure 4.1: Wind rose based on 30-minute data from May–October 2013–2020 at Kuivajärvi and frequency histogram based on daily mean values of wind speed for the same time period.

Intermonthly and interannual variation of wind speed was relatively small during the study period. Mean wind speeds during the individual May–October periods

from 2013 to 2020 were 1.92, 1.88, 1.96, 1.88, 2.06, 2.11, 1.99 and 2.13 m s^{-1}. Likewise the monthly variation was of the same magnitude, the mean wind speed being 2.11 m s^{-1} in May, 2.02 m s^{-1} in June, 1.89 m s^{-1} in July, 1.90 m s^{-1} in August, 1.95 m s^{-1} in September and 2.05 m s^{-1} in October, forming a pattern with slightly higher wind speeds towards start and end of the open water season (Fig. 4.2).

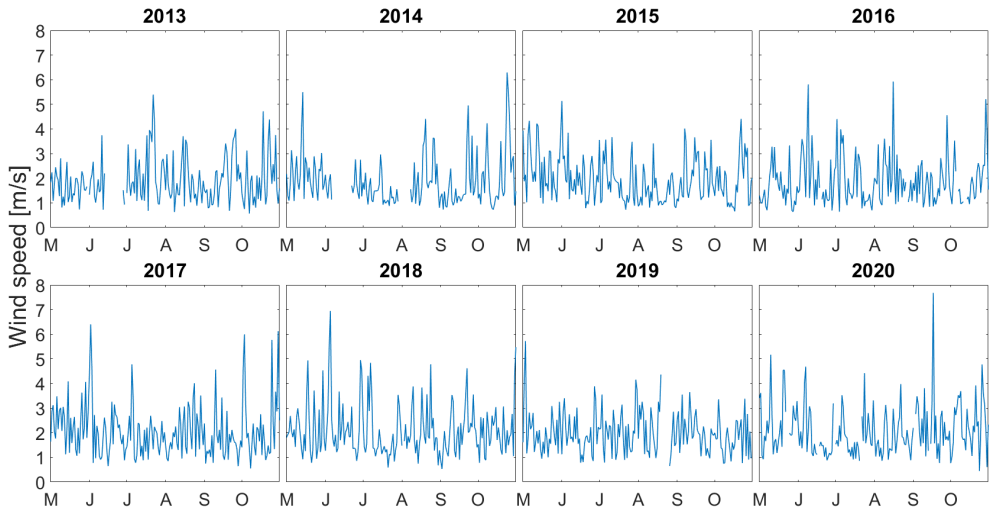

Figure 4.2: Daily mean wind speeds recorded at lake Kuivajärvi in May–October 2013–2020.

4.1.2 Air temperature and surface water temperature

Daily mean surface water temperature stayed above the daily mean air temperature for most of the time. Mean air temperatures for the individual May–October periods during the different years were 12.27 °C in 2013, 11.58 °C in 2014, 10.87 °C in 2015, 11.48 °C in 2016, 10.00 °C in 2017, 13.10 °C in 2018, 11.83 °C in 2019 and 11.93 °C in 2020. For comparison the 30-year mean (1981–2010) temperature for May–October period obtained from statistics (Pirinen, 2012) was 10.8 °C .

The annual maximums of daily mean surface water temperatures were 23.20 °C in 2013, 26.70 °C in 2014, 21.29 °C in 2015, 23.22 °C in 2016, 19.62 °C in 2017, 26.61 °C in 2018, 24.95 °C in 2019 and 25.98 °C in 2020. These values were reached in late July during the years 2014, 2016, 2018, 2019, early July in 2015 and already in the mid June in 2017 and in late June in 2013 and 2020.

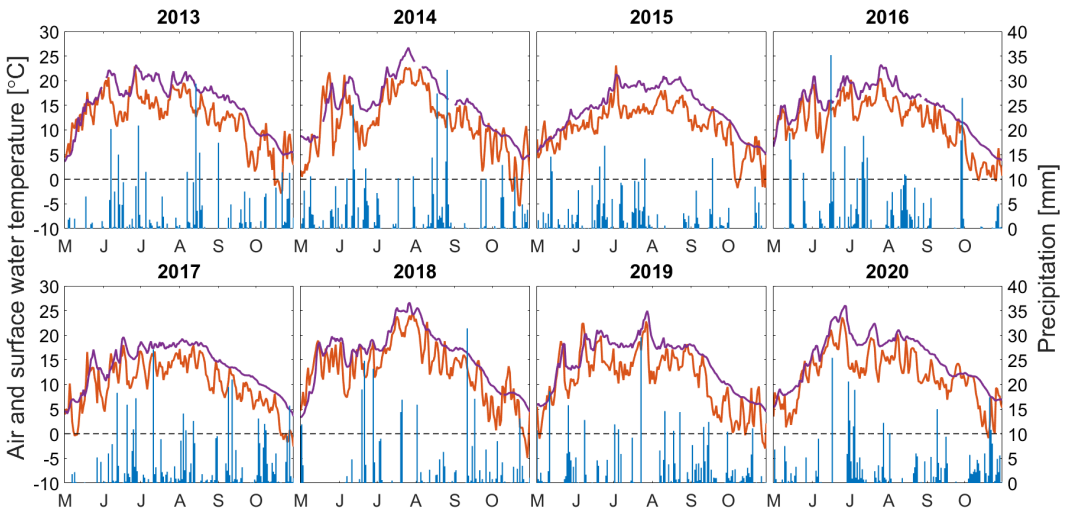

Figure 4.3: Daily mean air temperature (red line) and surface water temperature (purple line) with the daily sums of precipitation (blue bars) for the May–October 2013–2020 period.

4.1.3 Precipitation and snowmelt

Total precipitation during the May–October period varied from year to year, being lowest in 2015 with 289 mm and highest in 2017 with 430 mm, while the 30-year mean (1981-2010) precipitation for the May–October period in Hyytiälä was 433 mm (Pirinen, 2012). In terms of liquid precipitation the open water seasons analysed in this thesis were thus dryer than average, sum of precipitation for the May–October period being 345 mm in 2013, 392 mm in 2014, 289 mm in 2015, 382 mm in 2016, 430 mm in 2017, 317 mm in 2018, 356 mm in 2019 and finally 359 mm in 2020. More precise distribution of precipitation is given in the form of daily precipitation sums in Fig. 4.3. Total annual precipitation was 615 mm in 2013, 579 mm in 2014, 658 mm in 2015, 660 mm in 2016, 717 mm in 2017, 540 mm in 2018, 732 mm in 2019 and 677 mm in 2020, while the 30-year mean is 711 mm. Variation in the annual precipitation pattern affects the annual CO_2 emission, and to some extent, monthly mean values of surface water pCO_2 in finnish lakes (Rantakari and Kortelainen, 2005).

Snowmelt in spring produces another varying source of inflow to the lake. The evolution of snow water equivalent (SWE) in winter was also analysed, as in similar fashion to liquid precipitation, melting snow increases discharge and transport of terrestrial carbon into the lake. Evolution of SWE could possibly explain some of the large variation in measured values of pCO_2 during the spring peaks at Kuivajärvi. Large interannual variation in the evolution of SWE was observed between the

different study years, considering both the peak value and timing, and also the rate of eventual melting. In 2017–2018 peak SWE value in the approximate area around Kuivajärvi was 127 mm, occurring 1st of April, and falling to nearly zero before beginning of May. For comparison, in 2014 the peak value was only 13 mm, occurring already on the 16th of February. During the years with higher maximum values of SWE the maximum value was reached later in winter and decrease was considerably faster during melting in spring (Fig. 4.4). The years with maximum values of SWE, 2013 and 2018, also exhibited maximum peak values of surface pCO_2 at the beginning of May, which were 2919 μatm and 3105 μatm, respectively. Timing of carbon inputs into Kuivajärvi varies considerably based on the hydrological regime, high inputs coinciding with high discharge (Miettinen et al., 2020).

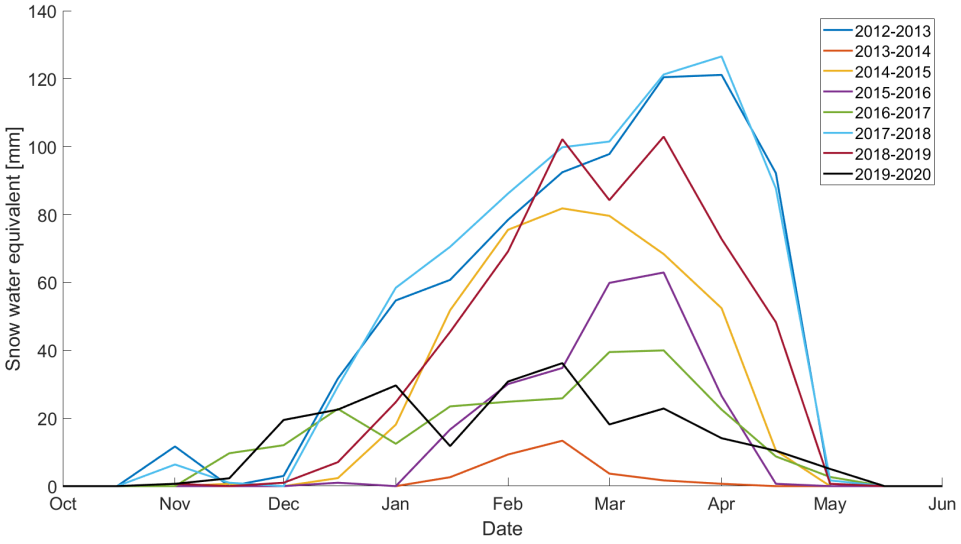

Figure 4.4: Evolution of snow water equivalent during the winters preceeding 2013–2020 open water periods.

4.1.4 Vertical thermal structure

Water column temperature followed typical seasonal pattern during the study period. The evolution of lake temperature structure during different years is revealed by water column contour plots based on daily mean temperatures (Fig. 4.5). Typically spring turnover ends and the stable summer stratification starts forming in May, ice-out having occurred earlier at some point during late April or very early May. However, the exact dates of ice-out in spring are not available. Initially thermal stratification is weak in spring and can still be largely eroded by varying weather

conditions, but as time progresses the stratification strenghtens and a period of permanent seasonal stratification follows. The seasonal thermocline is initially shallow, but deepens towards the end of summer, a development which can be identified during each of the study years. The seasonal thermocline is then ultimately eroded in autumn, allowing for complete lake turnover and deep mixing of the water column, which continues until ice-formation in winter.

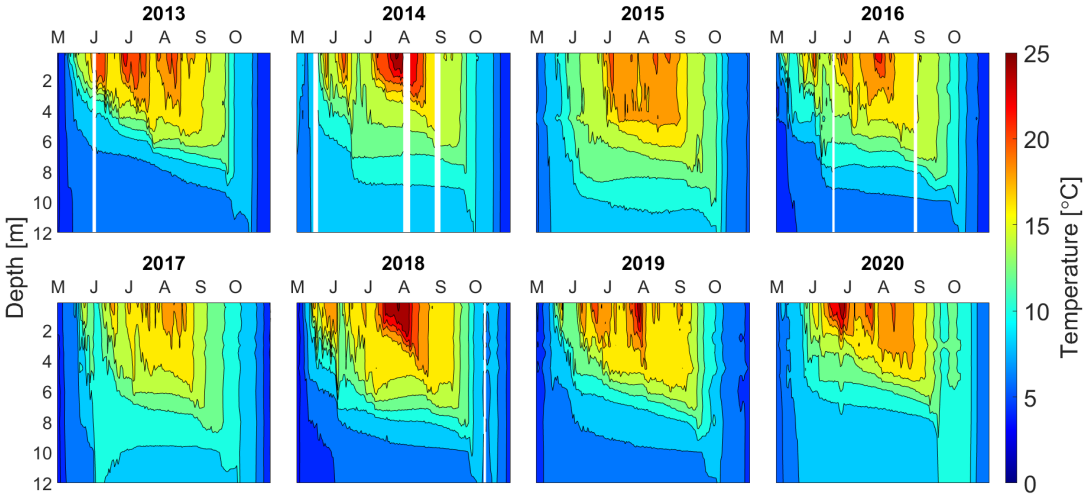

Figure 4.5: Contour plot of daily mean temperatures from May–October 2013–2020. Black lines represent 2 °C intervals and white space denotes gaps in the data.

Kuivajärvi exhibited dimictic behavior during the study period, which is evident from periods of uniform temperatures across the water column during spring and autumn. The spring turnover is noticeably shorter than autumn turnover, while it also exhibits large variation in timing and length between the different years. Annual surface water temperature maxima are most often accompanied by a relatively shallow and steep thermocline, as they occur during warm and calm periods.

There was noticeable variation in the evolution of vertical temperature structure between different years of the study period. Timing of stratification is strongly affected by the weather, and periods of strong wind and cold fronts weaken the stratification and enhance mixing of the water column, whereas calm and warm weather strenghtens the stratification. Strongest temperature gradients exist relatively close to the surface during warm summer periods, but permanent weaker temperature gradient is also present throughout most of the water column, save for the deepest part of the water column at and below approximately 10 m depth. This stable stratification structure exists throughout most of the open water season. Water column

temperature profile is of profound interest because it's the main cause of density variation in boreal lakes and is linked to the evolution of dissolved CO_2 in the water column.

4.1.5 Dissolved CO_2

Vertical pCO_2 profile

Water column pCO_2 shows the same type of general behavior throughout different years of the study (Fig. 4.6). At the start and towards the end of the open water season pCO_2 values at different depths in the water column are almost equal, while there are large differences between different measurement depths during the stable stratification in summer. The water column is mixed during spring and autumn turnovers, which leads to the nearly uniform vertical pCO_2 profile in the lake. However, as soon as stable stratification develops after the spring turnover, hypolimnion becomes insulated from exchanging CO_2 with the surface, leading to accumulation of CO_2 due to still ongoing respiration processes in the deeper parts of the lake. Photosynthetic activity and CO_2 exchange between water surface and atmosphere cause decrease in pCO_2 values in the epilimnion during stratification. The accumulated CO_2 in the hypolimnion is vented in autumn once the lake turnover reaches deep enough, observable from the rapid decrease in measured pCO_2 values at 7 m depth and increase at the surface and shallower measurement points. The peak values of pCO_2 at 7 m depth are relatively similar during different years, but there is inter-annual variation in the accumulation rate and timing. During years with rapid development of stable stratification the accumulation of CO_2 occurs over longer time but at a slower rate. During years with extended mixing pCO_2 values are lower during early part of the open water season, but the accumulation is faster later on. This could be explained by warmer hypolimnetic temperatures leading to increased rate of microbial production of CO_2 (Mammarella et al., 2018).

Measured values of pCO_2 at the surface and 1.5 m depth are strongly correlated ($r = 0.84$). Additionally pCO_2 at 2.5 m measurement depth is still moderately correlated ($r = 0.43$) with the values at the surface, but there are already signs of decoupling, probably due to the effect of stratification. Finally, during the stratified period the evolution of pCO_2 at the deepest measurement point at 7 m is clearly decoupled from the surface ($r = -0.14$).

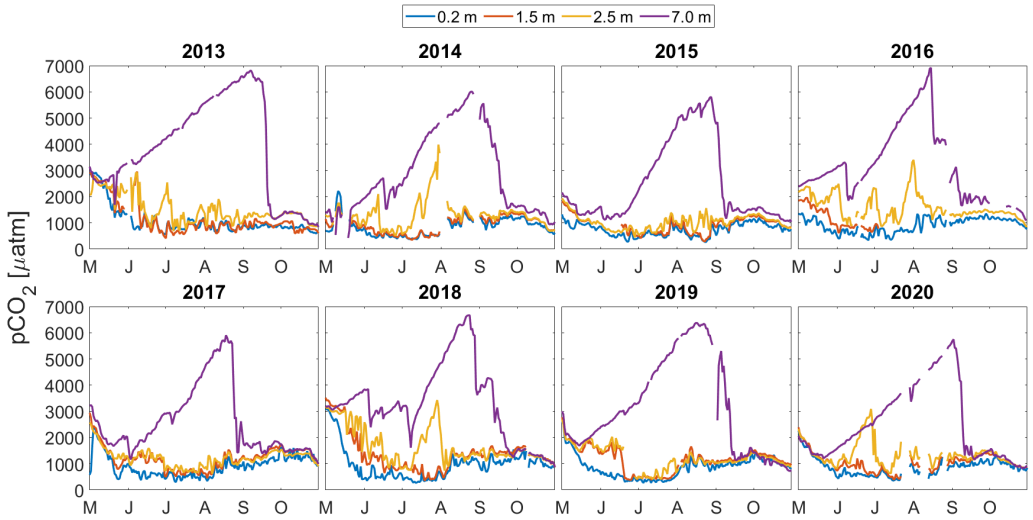

Figure 4.6: Daily mean pCO_2 at different depths during May–October 2013–2020.

Surface water pCO_2

Development of surface water pCO_2 during the May–October periods is shown in Fig. 4.7. It's evident that the pCO_2 variation between different study years is largest during the spring, and it follows more predictable pattern during the summer and autumn. The maximum values of surface water pCO_2 were reached in spring and the minimum in the middle of summer. In addition to the peak in spring the surface pCO_2 exhibited another smaller and broader peak in autumn.

Explanations for the large peaks in spring are terrestrial carbon inputs to the lake from the surrounding area especially during the spring freshet, but also gradually during the winter (Miettinen et al., 2020). Another possible reason for the accumulation of CO_2 is continuing degradation of organic matter during the ice cover. The accumulated CO_2 is rapidly released after ice-out in spring, and as the time progresses stable stratification is formed, resulting in insulation of the surface layer from the deeper parts of the lake, which leads to sharp decrease in surface pCO_2 and the minimum reached in summer. Autumn peak is later caused by water column mixing during the turnover and the CO_2 accumulated in the hypolimnion during the summer being vented to the surface.

Surface waters of Kuivajärvi remain supersaturated with CO_2 throughout the vast majority of the open water season, but in the middle of summer pCO_2 at the surface can be close to atmospheric values, and possibly momentarily even below them. The maximum value of daily mean surface water pCO_2 during the study period was 3105 μatm, which was reached in early May in 2018. The minimum was

270 μatm, measured during July in 2019. During the years 2015, 2016 and 2020 the maximum surface pCO_2 value during the spring peak was reached already in late April.

While the surface water pCO_2 at Kuivajärvi exhibits behavior with peaks both during spring and autumn, the peaks are fundamentally different in their nature. The spring peak is considerably higher, steeper and more variable, while the autumn peak is quite moderate, predictable and broad. This causes difficulties for the use of a water column stability based proxy in predicting pCO_2, as the stratification in both cases is very weak, but values of pCO_2 different. Same kind of behavior in Kuivajärvi with larger spring peak of surface CO_2 was also presented in the paper (Miettinen et al., 2015) for the years 2011 and 2012.

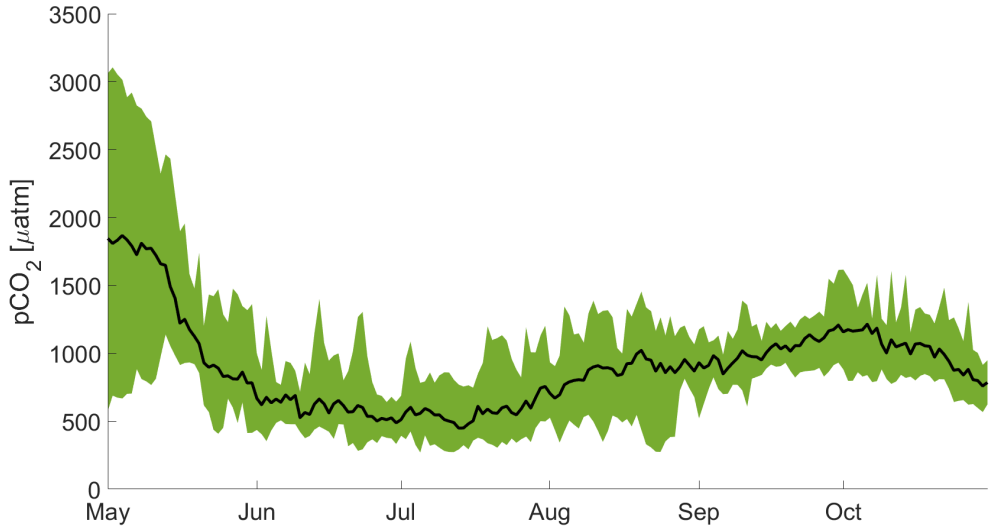

Figure 4.7: Variation of daily mean lake surface pCO_2 during May–October 2013–2020. Black line represents mean of daily mean pCO_2 values measured at that time of year and the green shaded area outlines total variation from maximum to minimum.

4.2 Relationship between Brunt-Väisälä frequency and surface water pCO_2

4.2.1 N as a proxy for surface water pCO_2

Relationship between N, which was calculated over varying depth intervals (Eq. 3.1), and surface water pCO_2 was evaluated during the 8 consecutive May–October

periods in 2013–2020. Evolution of N calculated from few of these depth intervals is shown in Fig 4.8. Daily mean values of N calculated from 4 m or shallower depth intervals occassionally reach close to zero values during momentary periods of cooling and mixing, while the resulting pCO_2 increase at the surface due to mixing is nowhere near as drastic as these changes in N. This would suggest optimal lower boundary for N calculation below the 4 m depth. Lower bounds of depth interval down from 8 meters result in N values which follow each other closely during most of the May–October period, but exhibit some differences at the end of summer depending on rapidity of the thermocline deepening and erosion before autumn turnover.

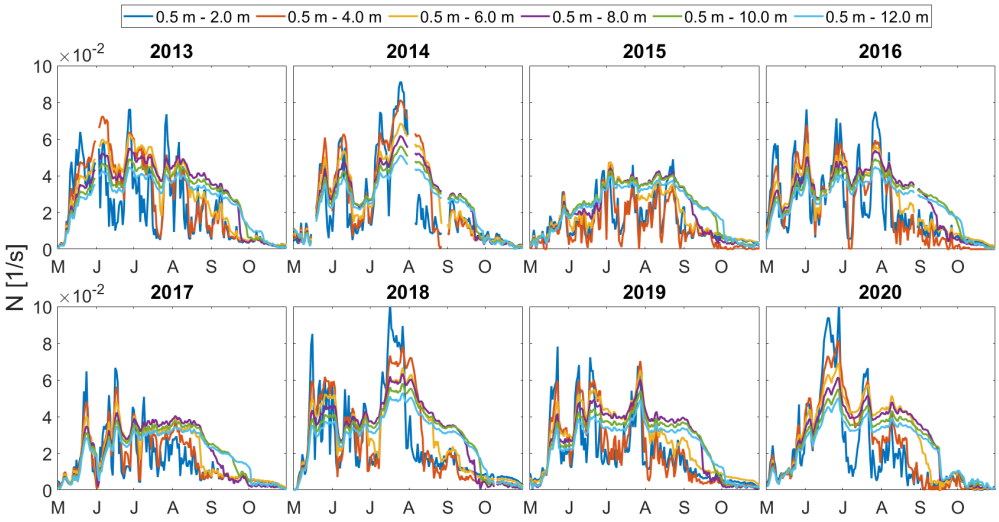

Figure 4.8: Daily mean values of N calculated from 6 different depth intervals during the May–October 2013–2020 study period.

It's clear that the optimal choice for lower boundary of depth interval when calculating N is deeper at Kuivajärvi than the 1.5 m suited for Valkea-Kotinen (Huotari et al., 2009, 2011). This is probably caused by the several key differences in the two lake's characteristics such as water transparency, surface area, shape and depth, while there are also differences in the surrounding catchment areas of the lakes. However, the lakes are located relatively close to each other with Valkea-Kotinen residing roughly 80 km southeast of Kuivajärvi, so there shouldn't be notable climate related disparities between them.

Choosing too shallow lower boundary for calculation of N results in too low values in a case where the main thermocline is partially or completely below that depth, while a depth interval reaching too deep could result in issues with interpre-

tation, as different cases with completely different characteristics can result in the same value for N. There can be a steep and shallow thermocline resulting in the same value for N as a rather uniform temperature gradient across the water column. This seems to pose a challenge for the method at Kuivajärvi, as thermocline deepens considerably towards the end of summer, and the stratification structure can also otherwise vary due to weather events. Temperature data from every available measurement depth was analyzed to find a depth interval resulting in the best possible fit between N and surface water pCO_2 values. For the lower boundary of N calculation each of the measurement depths below 0.5 m was considered, and for the upper boundary 0.2 m and 0.5 m, both yielding similar results in general. However, the temperature measured at 0.2 m depth was occasionally below the measurement at 0.5 m and even some of the other depths, which probably stemmed from inaccuracy of the measurement instruments.

Pearson correlation was used alongside curve fitting in assessing viability of different depth intervals for N, and the values of correlation coefficient r for 0.5 m upper depth interval limit with varying lower depth intervals are shown in table 4.1 for both N and pCO_2 (μatm), and N and CO_2 concentration (μmol/l). Difference in the relationships is explained by pCO_2 being affected by temperature, as solubility of CO_2 in water decreases with increasing temperature, resulting in increase in the partial gas pressure. CO_2 concentration represents the amount of CO_2 in molecules in the given space and is unaffected by changing temperature. However, this difference has no meaningful effect on the final results, as the predicted pCO_2 values will be anyways transformed into CO_2 concentration for the flux calculation (Eq. 2.3). Both are shown to improve interpretability of the results.

Notable inter-annual variations in the relationship between N and surface water pCO_2 were recorded as illustrated in Fig. 4.9. Both of the years 2015 and 2016 were characterized by lower than average surface pCO_2 values in May if compared to the other years. During 2015 the water column was less stable, but during both years N and surface water pCO_2 exhibited similar relationship, which was best described by a linear fit. In turn, the years 2017, 2019 and 2020 were characterized by the relationship between N and surface water pCO_2 most closely resembling exponential decay in shape. In 2014 the fit between N and pCO_2 was rather poor overall, with pCO_2 values not meaningfully being affected by changes in N during entirity of June and July. Finally the relationship between N and pCO_2 during of 2013 and 2018 was initially similar, both years being characterized by high surface pCO_2 values in May, which were followed by a linear descent as stable stratification

N vs pCO_2

Depth interval [m] used in N calculation	2013	2014	2015	2016	2017	2018	2019	2020	2013-2020
0.5-1.0	-0.03	-0.43	-0.67	-0.50	-0.65	-0.26	-0.49	-0.41	-0.32
0.5-1.5	0.02	-0.46	-0.64	-0.60	-0.54	-0.33	-0.53	-0.51	-0.35
0.5-2.0	0.00	-0.51	-0.68	-0.65	-0.61	-0.43	-0.50	-0.54	-0.38
0.5-2.5	-0.06	-0.53	-0.71	-0.67	-0.70	-0.49	-0.57	-0.58	-0.42
0.5-3.0	-0.07	-0.51	-0.72	-0.68	-0.69	-0.48	-0.55	-0.58	-0.41
0.5-3.5	-0.10	-0.50	-0.68	-0.69	-0.70	-0.49	-0.64	-0.63	-0.42
0.5-4.0	-0.10	-0.49	-0.67	-0.70	-0.70	-0.48	-0.65	-0.66	-0.42
0.5-4.5	-0.13	-0.48	-0.62	-0.71	-0.71	-0.46	-0.68	-0.68	-0.41
0.5-5.0	-0.14	-0.47	-0.73	-0.68	-0.73	-0.50	-0.74	-0.69	-0.46
0.5-6.0	-0.19	-0.46	-0.71	-0.67	-0.74	-0.53	-0.79	-0.69	-0.48
0.5-7.0	-0.25	-0.44	-0.71	-0.65	-0.75	-0.57	-0.75	-0.68	-0.49
0.5-8.0	-0.28	-0.44	-0.71	-0.62	-0.75	-0.58	-0.73	-0.68	-0.50
0.5-10.0	-0.31	-0.44	-0.69	-0.55	-0.75	-0.59	-0.73	-0.68	-0.51
0.5-12.0	-0.34	-0.43	-0.65	-0.54	-0.73	-0.60	-0.72	-0.69	-0.51

N vs CO_2 concentration

Depth interval [m] used in calculation of N	2013	2014	2015	2016	2017	2018	2019	2020	2013-2020
0.5-1.0	-0.21	-0.58	-0.75	-0.61	-0.65	-0.33	-0.53	-0.41	-0.41
0.5-1.5	-0.14	-0.58	-0.73	-0.61	-0.51	-0.37	-0.58	-0.54	-0.42
0.5-2.0	-0.15	-0.61	-0.72	-0.71	-0.59	-0.45	-0.53	-0.54	-0.44
0.5-2.5	-0.23	-0.64	-0.78	-0.77	-0.71	-0.52	-0.61	-0.59	-0.49
0.5-3.0	-0.23	-0.64	-0.77	-0.76	-0.67	-0.50	-0.56	-0.58	-0.47
0.5-3.5	-0.27	-0.65	-0.68	-0.77	-0.71	-0.52	-0.66	-0.65	-0.49
0.5-4.0	-0.27	-0.65	-0.72	-0.78	-0.69	-0.51	-0.66	-0.67	-0.50
0.5-4.5	-0.29	-0.65	-0.68	-0.78	-0.71	-0.50	-0.67	-0.71	-0.50
0.5-5.0	-0.31	-0.66	-0.80	-0.80	-0.73	-0.55	-0.75	-0.72	-0.55
0.5-6.0	-0.37	-0.66	-0.82	-0.83	-0.76	-0.59	-0.82	-0.74	-0.59
0.5-7.0	-0.43	-0.67	-0.83	-0.83	-0.78	-0.64	-0.81	-0.75	-0.62
0.5-8.0	-0.47	-0.68	-0.85	-0.84	-0.79	-0.65	-0.81	-0.76	-0.64
0.5-10.0	-0.50	-0.68	-0.86	-0.82	-0.81	-0.68	-0.82	-0.76	-0.66
0.5-12.0	-0.52	-0.67	-0.84	-0.81	-0.81	-0.69	-0.83	-0.77	-0.66

Table 4.1: Pearson correlation between daily means of N and surface pCO_2 (upper) and between N and surface CO_2 concentration (lower) for the May–October period during individual years and all study period. Upper N depth interval boundary of 50 cm resulted in slightly better results overall and is thus shown.

developed. This same kind of behavior during stability formation in spring was also reported by Huotari et al. (2009) at Valkea-Kotinen, where a linear relationship was initially observed between N and pCO_2 concentration after the peak in spring, but later observations were better described by an exponential decay fit. Oddly enough during 2013 the expected increase in surface pCO_2 during mixing in autumn wasn't observed, contrary to all other years. This resulted in close to non-existent correlation between pCO_2 and N for the shorter depth intervals, and poor correlation for the longer ones (Table 4.1).

As there were large differences in the relationship of N and pCO_2 between

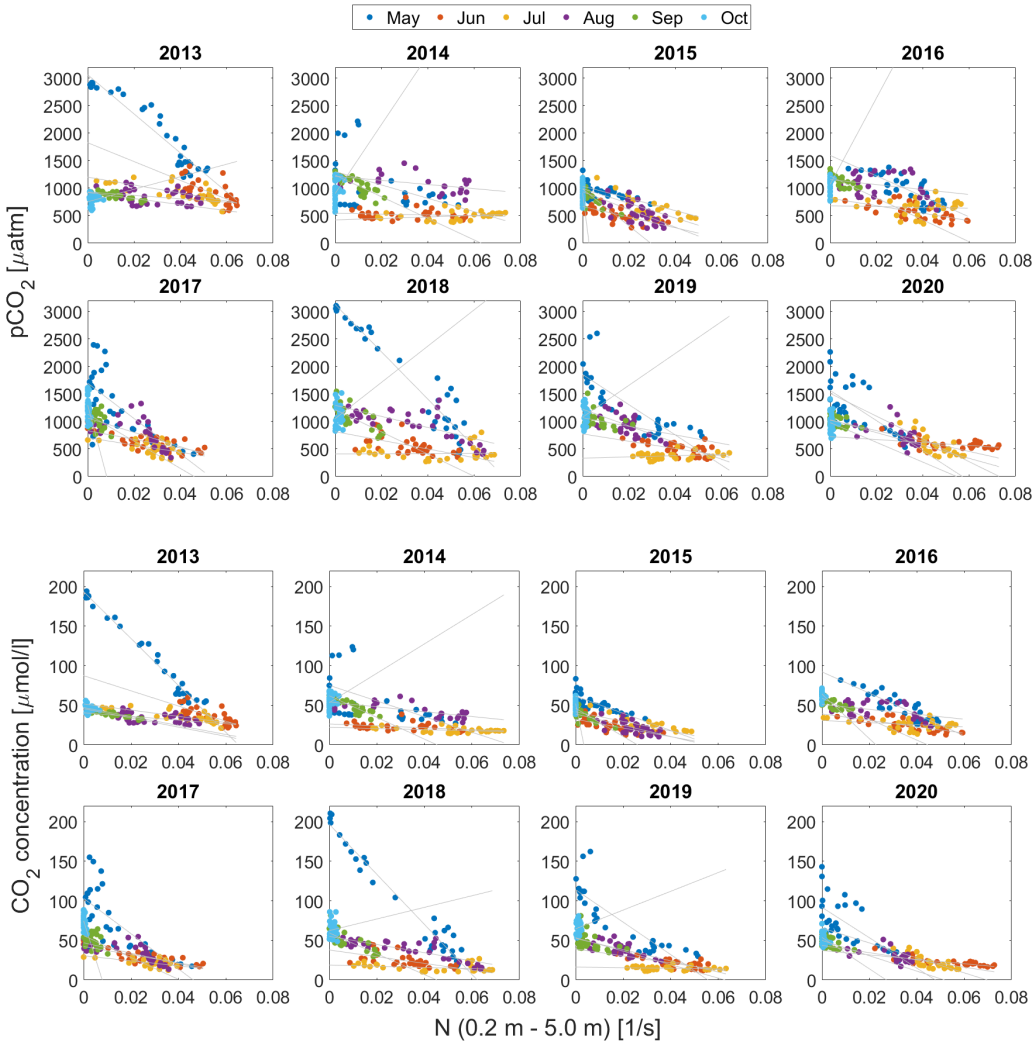

Figure 4.9: Scatter plots of N (20 cm – 500 cm) and both surface pCO_2 and CO_2 concentration during different years.

different analysed years, a depth interval for N calculation and fit between the variables providing good results during one year might yield bad results for other years. As shown earlier in Fig. 4.7, the surface pCO_2 values varied by a large margin between the springs. However, the water column stability conditions and thus values of N could be very much alike during these periods. This and the earlier mentioned characteristics reduced the overall goodness of fit between N and surface water pCO_2 during the 2013–2020 study period. The relationship between daily mean values of N and surface water pCO_2 for all study period was best described by a linear fit with N calculation depth interval spanning across the entirity of the water column, which is shown in Fig. 4.10, where the measurements done during May are separated from the rest by color. This fit resulted in Eq. 4.1

$$\mathrm{pCO_2} = -16020N + 1284 \tag{4.1}$$

which was used to predict surface $\mathrm{pCO_2}$ for the BLM flux calculation via Eq. 2.3. The R^2 values in Fig. 4.10 correspond to r values of 0.51 and 0.66 for $\mathrm{pCO_2}$ and $\mathrm{CO_2}$ concentration, respectively. When the $\mathrm{pCO_2}$ predicted by Eq. 4.1 was transformed into $\mathrm{CO_2}$ concentration and compared with the $\mathrm{CO_2}$ concentration values obtained from the measurements a slightly higher value for Pearson correlation was obtained ($r = 0.68$). Also Huotari et al. (2011) observed a linear relationship between N and $\mathrm{pCO_2}$ at Valkea-Kotinen when analyzing combined data from several years.

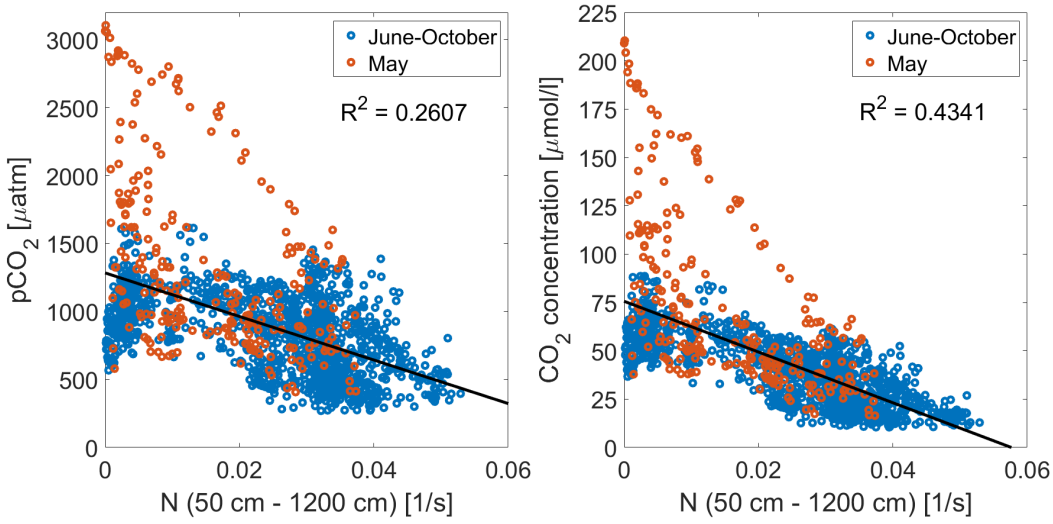

Figure 4.10: Best fits for daily mean N and both surface $\mathrm{pCO_2}$ and $\mathrm{CO_2}$ concentration during the complete May–October 2013–2020 study period. Data from May deviated noticeably from rest of the measurements and is highlighted in red color.

Relationship between N and surface water $\mathrm{pCO_2}$ in June–October

It was additionally noted that while the fit between N and surface water $\mathrm{pCO_2}$ wasn't particularly good when analyzing the 8 consecutive May–October periods as a whole, ignoring the measurements made during May resulted in shortening of the optimal depth interval for N and the goodness of fit increasing noticeably. Additionally upper depth boundary of 20 cm for N calculation yielded better results than 50 cm. Pearson correlation between N and $\mathrm{pCO_2}$, and N and $\mathrm{CO_2}$ concentration for the June–October period are shown in Table 4.2. This change also resulted in the relationship between the variables shifting to more closely resemble exponential

decay instead of linear decrease. The improved relationship could suggest that the surface water pCO_2 is indeed largely controlled by changes in water column stability at Kuivajärvi, but only outside the peak occurring in spring during ice-out and lake turnover, which is when other factors also play a major role. It should be kept in mind that the relationship between N and pCO_2 is still generally strongly negative during May, but this relationship doesn't fit the same simple N based model very well.

N vs pCO_2

Depth interval [m] used in N calculation	2013	2014	2015	2016	2017	2018	2019	2020	2013-2020
0.2-0.5	-0.16	-0.42	-0.37	-0.44	-0.43	-0.53	-0.27	-0.59	-0.37
0.2-1.0	-0.11	-0.55	-0.55	-0.59	-0.56	-0.55	-0.44	-0.61	-0.45
0.2-1.5	-0.15	-0.57	-0.62	-0.70	-0.59	-0.62	-0.61	-0.65	-0.54
0.2-2.0	-0.17	-0.63	-0.67	-0.73	-0.65	-0.70	-0.58	-0.69	-0.57
0.2-2.5	-0.16	-0.64	-0.73	-0.76	-0.72	-0.71	-0.65	-0.73	-0.58
0.2-3.0	-0.11	-0.60	-0.72	-0.77	-0.77	-0.74	-0.65	-0.73	-0.59
0.2-3.5	-0.05	-0.58	-0.72	-0.76	-0.74	-0.72	-0.76	-0.77	-0.58
0.2-4.0	-0.04	-0.56	-0.70	-0.76	-0.79	-0.72	-0.77	-0.80	-0.59
0.2-4.5	-0.01	-0.54	-0.63	-0.77	-0.80	-0.68	-0.80	-0.81	-0.57
0.2-5.0	0.01	-0.53	-0.74	-0.73	-0.81	-0.70	-0.84	-0.81	-0.60
0.2-6.0	0.09	-0.50	-0.72	-0.70	-0.81	-0.68	-0.85	-0.78	-0.59
0.2-7.0	0.13	-0.47	-0.70	-0.67	-0.81	-0.68	-0.77	-0.74	-0.57
0.2-8.0	0.14	-0.45	-0.69	-0.62	-0.81	-0.65	-0.73	-0.72	-0.56
0.2-10.0	0.15	-0.43	-0.64	-0.53	-0.79	-0.61	-0.70	-0.70	-0.53
0.2-12.0	0.15	-0.41	-0.59	-0.51	-0.75	-0.60	-0.68	-0.70	-0.51

N vs CO_2 concentration

Depth interval [m] used in N calculation	2013	2014	2015	2016	2017	2018	2019	2020	2013-2020
0.2-0.5	-0.47	-0.48	-0.38	-0.47	-0.39	-0.51	-0.29	-0.63	-0.41
0.2-1.0	-0.60	-0.66	-0.57	-0.63	-0.54	-0.58	-0.46	-0.65	-0.53
0.2-1.5	-0.59	-0.69	-0.65	-0.72	-0.56	-0.63	-0.67	-0.73	-0.61
0.2-2.0	-0.64	-0.73	-0.69	-0.77	-0.63	-0.70	-0.61	-0.75	-0.64
0.2-2.5	-0.68	-0.77	-0.78	-0.85	-0.74	-0.75	-0.71	-0.79	-0.68
0.2-3.0	-0.64	-0.77	-0.77	-0.83	-0.76	-0.78	-0.67	-0.77	-0.68
0.2-3.5	-0.63	-0.77	-0.75	-0.83	-0.76	-0.77	-0.80	-0.85	-0.69
0.2-4.0	-0.63	-0.76	-0.74	-0.84	-0.79	-0.78	-0.78	-0.87	-0.70
0.2-4.5	-0.62	-0.76	-0.67	-0.84	-0.81	-0.76	-0.79	-0.89	-0.69
0.2-5.0	-0.63	-0.76	-0.83	-0.85	-0.83	-0.80	-0.87	-0.90	-0.74
0.2-6.0	-0.62	-0.75	-0.84	-0.87	-0.86	-0.82	-0.91	-0.91	-0.76
0.2-7.0	-0.65	-0.75	-0.84	-0.86	-0.88	-0.85	-0.89	-0.90	-0.78
0.2-8.0	-0.66	-0.75	-0.85	-0.86	-0.88	-0.84	-0.88	-0.89	-0.78
0.2-10.0	-0.66	-0.73	-0.85	-0.82	-0.89	-0.82	-0.87	-0.88	-0.78
0.2-12.0	-0.66	-0.72	-0.81	-0.81	-0.87	-0.81	-0.86	-0.88	-0.77

Table 4.2: Pearson correlation between N and pCO_2 (upper), and N and CO_2 concentration (lower) for June–October period during individual years and all study period. Upper N depth interval boundary of 20 cm resulted in slightly better results for the June–October period and is thus shown.

Monthly mean values of N and surface water pCO_2

Averaging the data to monthly values leads to somewhat better results with the shorter depth intervals for N calculation. This change could stem from short-lived erosion of shallow stratification not resulting in the value of N for the period being reduced to zero. As can be expected, the averaging also improved the correlation between N and surface water pCO_2. Additionally when considering only the June–October instead of the complete measurement period, the best fit between N and pCO_2 resembles exponential decay and is obtained by using N from as shallow depth interval as 0.2 m to 2.0 m, illustrated in Fig. 4.11.

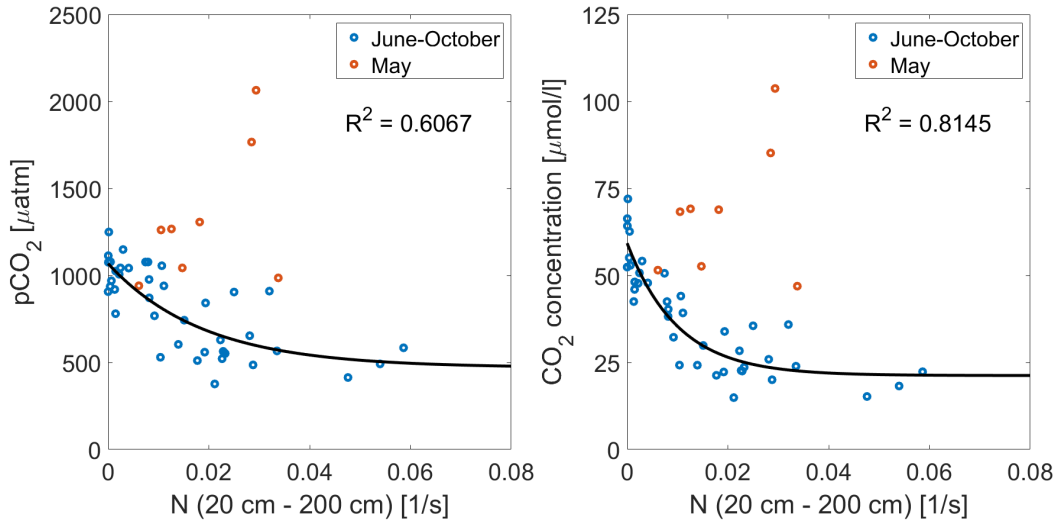

Figure 4.11: Scatter plots of monthly mean N (20 cm – 200 cm), and both pCO_2 and CO_2 concentration. Data from May is shown in red but is not part of the fit.

4.2.2 Comparison to earlier studies promoting feasibility of Brunt-Väisälä frequency based proxy for dissolved CO_2

Earlier observations on boreal lakes have shown that dissolved CO_2 at the lake surface follows a cycle with peaks in spring and autumn, while the relationship between surface water CO_2 and N was evaluated at lake Valkea-Kotinen by Huotari et al. (2009, 2011). In the earlier paper a connection between water column stability described by N, calculated from 0.5 m to 1.5 m depth interval, and surface water CO_2 concentration (μmol/l) was found and best described by fitting an exponential decay curve. In Huotari et al. (2011) a linear relationship between monthly mean N,

calculated between 0.2 m and 1.5 m depths, and surface water pCO_2 values from a time period spanning 5 years was shown. It should be noted that the surface water pCO_2 and CO_2 concentration are interchangeable via the use of Henry's law.

The exponential fit in Huotari et al. (2009) was shown for the relationship between N and CO_2 concentration for the open water period of year 2006. However, it is noted that during the six initial days of developing stable stratification in spring the relationship between surface water CO_2 concentration and N appears to be linearly instead of exponentially decreasing. The goodness of fit, R^2, for the equation was 0.71, indicating a strong relationship between the variables. However, this was only shown for data measured during a single open water season in 2006. In the paper Huotari et al. (2011) R^2 for the linear fit between monthly mean values of N and surface water pCO_2 during the open water seasons of years 2003–2007 was 0.765, again promoting a strong relationship between the two variables.

Apparently the different characteristics between the two lakes lead to the relationship between N and surface water CO_2 at lake Kuivajärvi not being as straightforward as at Valkea-Kotinen. Kuivajärvi is considerably deeper with a maximum depth of 13.2 m compared to 6.5 m at Valkea-Kotinen, while the mean depths are 6.5 m and 2.5 m, respectively. The surface area of Kuivajärvi is around 0.62 km^2 compared to 0.041 km^2 at Valkea-Kotinen and the shape of Kuivajärvi is more oblong. Being better sheltered from the wind helps Valkea-Kotinen to develop stronger stable near surface conditions, which in turn can promote phytoplankon growth and prevent a shallow surface layer from receiving CO_2 from deeper parts of the water column. At Kuivajärvi the mixing depth often reaches below the illuminated layer, which has a negative effect on photosynthesis by phytoplankton (Miettinen et al., 2015). Water transparency affects absorbtion of solar radiation in the water column and probably also plays a role in causing differences in stratification conditions between the lakes. Valkea-Kotinen is less transparent with a Secchi depth of around 1 m (Arst et al., 2008), while in Kuivajärvi values between 1.2 m and 1.5 m are typically measured (Heiskanen et al., 2015).

In addition to the effects of differing water column stratification structure, a key difference seems to be the relative importance of the spring peak of surface water CO_2. At Kuivajärvi the spring peak is more prominent and seems to be responsible for larger part of annual CO_2 flux, whereas at Valkea-Kotinen autumn peak is relatively more important. This could result from the incomplete turnovers at Valkea-Kotinen (Huotari et al., 2009, 2011) in spring in contrast to the complete turnovers at the dimictic Kuivajärvi, leading to reduction in size of the spring peak

at Valkea-Kotinen. As the amount of released CO_2 in Valkea-Kotinen is smaller during spring, the lower part of the water column stores excess CO_2 until release later during the autumn turnover, which increases the size of the autumn surface water CO_2 peak. The lake turnover related CO_2 peaks in spring and autumn being closer to each other in magnitude in Valkea-Kotinen than in Kuivajärvi might also be the reason for N seeming more feasible as a proxy for the surface water CO_2 at Valkea-Kotinen, as the water column stability conditions are similar during both turnovers.

4.3 Comparison of CO_2 fluxes obtained via different methods

4.3.1 Comparison between CO_2 fluxes calculated from measurements and proxy

CO_2 flux was calculated from the pCO_2 values predicted by Eq 4.1 according to Eq. 2.3 and the results are illustrated in Fig. 4.12. While the flux of CO_2 obtained with use of the proxy exhibited same kind of seasonal cycle with higher fluxes in spring and autumn with considerably smaller fluxes in the middle of summer, the magnitude of the peaks wasn't very well represented. As could be expected based on the prior analysis in this thesis, the proxy fails to capture the highest peaks of pCO_2 in spring. Otherwise the proxy yields better results, but still tends to underestimate pCO_2 values during early half of the autumn peak, while being prone to overestimation during middle of summer and at the end of autumn peak. Flux during these later mentioned time periods could be better described by a proxy based on data from the June-October period, during which N and surface pCO_2 had a stronger relationship. However this would severely diminish any usefulness the proxy may have, as the spring peak can be responsible for a large fraction of the annual flux and cannot be ignored. Pearson correlation between the CO_2 flux calculated based on the pCO_2 measurements and the one calculated from the proxy was 0.62 for all 2013–2020 study period, and for such a simple proxy this could be interpreted as a rather good result.

However, correlation between these CO_2 fluxes is slightly worse than could be expected based solely on the relationship ($r = 0.68$) between the predicted and measured pCO_2 values after they're transformed into CO_2 concentrations for the flux calculation. Same gas transfer velocity is used in both flux calculations (Eq. 2.4),

which should improve the correlation between the fluxes. The lower correlation between the CO_2 fluxes if compared to the CO_2 concentrations is explained by the magnitude and direction of the flux being governed by the difference between surface CO_2 concentration (C_{sur}) and equilibrium concentration in air (C_{eq}) (Eq. 2.3), instead of just the absolute value of C_{sur} alone. This can lead to situations where relatively small initial differences in the predicted and measured pCO_2 values cause the calculated fluxes to have large differences in relative magnitude when the values for C_{sur} are close to C_{eq}, and even opposite flux directions occasionally occur in summer.

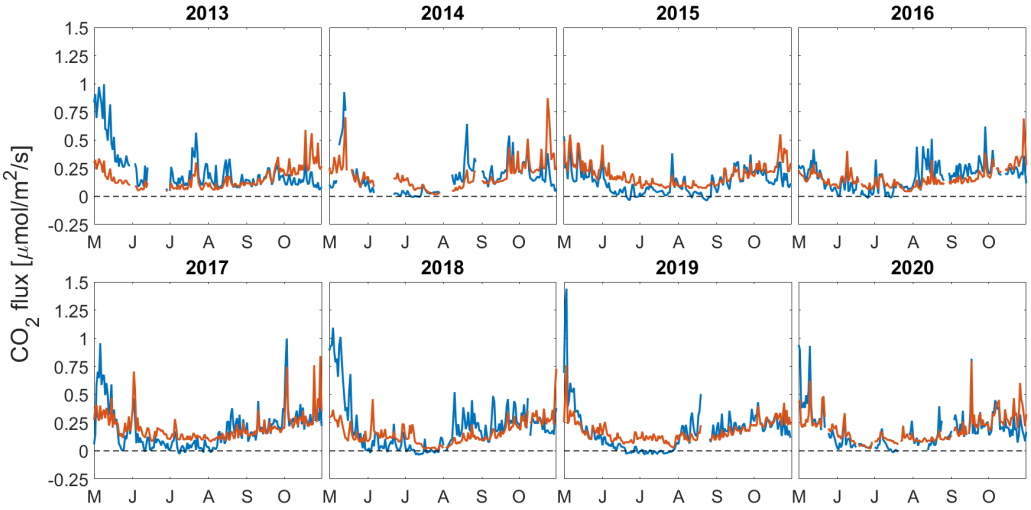

Figure 4.12: Daily mean CO_2 flux calculated from pCO_2 values predicted by the proxy (red) and from the measurements (blue).

Mean monthly CO_2 fluxes during the 2013–2020 study period based on the proxy were 0.23 μmol m^{-2} s^{-1} in May, 0.14 μmol m^{-2} s^{-1} in June, 0.10 μmol m^{-2} s^{-1} in July, 0.11 μmol m^{-2} s^{-1} in August, 0.18 μmol m^{-2} s^{-1} in September and 0.30 μmol m^{-2} s^{-1} in October. For comparison fluxes based on the pCO_2 measurements were 0.34 μmol m^{-2} s^{-1} in May, 0.07 μmol m^{-2} s^{-1} in June, 0.06 μmol m^{-2} s^{-1} in July, 0.17 μmol m^{-2} s^{-1} in August, 0.22 μmol m^{-2} s^{-1} in September and finally 0.22 μmol m^{-2} s^{-1} in October.

4.3.2 Comparison of eddy covariance and boundary layer method fluxes

Finally a comparison was made between monthly mean CO_2 fluxes obtained via three different methods: BLM using both pCO_2 obtained from the N based proxy

and the direct measurements, and the EC measurements done at the raft (Fig. 4.13). As can be expected, values obtained from both BLM options followed each other relatively closely. However, there was a large difference between BLM and EC fluxes. Besides the magnitude there was also a notable difference between timing of the peak fluxes during some of the years, as the flux peaks in spring and autumn clearly visible in results of BLM are not as evident in the EC data.

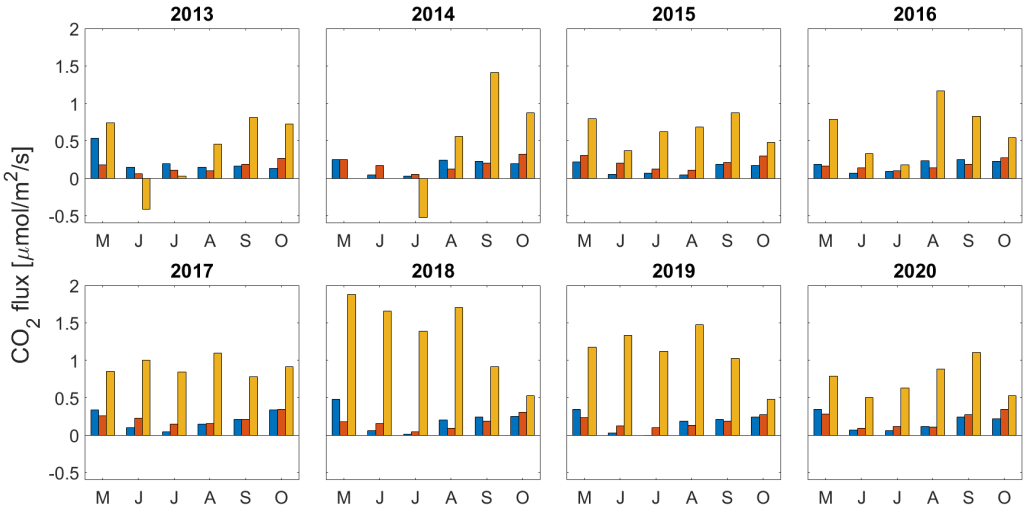

Figure 4.13: Comparison between monthly mean CO_2 fluxes from BLM based on the measurements (blue) and proxy (red), and EC (yellow) during the May–October 2013–2020 study period.

Monthly mean fluxes based on EC data with quality flag 0 (very good) were 1.33 μmol m^{-2} s^{-1} in May, 0.95 μmol m^{-2} s^{-1} in June, 0.81 μmol m^{-2} s^{-1} in July, 1.26 μmol m^{-2} s^{-1} in August, 1.13 μmol m^{-2} s^{-1} in September and 0.72 μmol m^{-2} s^{-1} in October.

The large observed differences between the modelled and EC fluxes are related to k parametrisation. The use of solely wind speed based model for k results in too low flux estimates for Kuivajärvi, while more complex models would give better results. For details see Heiskanen et al. (2014). Similar, albeit smaller, differences between BLM and EC were recorded in Kuivajärvi earlier by Erkkilä et al. (2018) when comparing fluxes for a relatively short period consisting of both stratified and mixing period in autumn. It was also reported by Mammarella et al. (2015) that the wind speed based k_{CC} strongly underestimated the CO_2 flux in Kuivajärvi in 2010 and 2011, while k parametrisation including the buoyancy flux gave better results.

5. Conclusions

The relationship between N and surface water pCO_2 was studied in lake Kuivajärvi in order to evaluate the viability of a water column stratification parameter as a proxy for surface water pCO_2. Study period consisted of 8 consecutive May–October periods between 2013 and 2020. The N based proxy was used to estimate CO_2 flux with BLM and the result was evaluated against flux based on the same method and measured values of pCO_2. These modelled fluxes were also compared to the flux obtained from EC measurements.

Daily mean values of N and pCO_2 were moderately or even strongly negatively correlated during each individual year except for 2013, during which the expected autumn peak of surface pCO_2 was not observed. The relationship during all study period was best described by a linear fit and N calculation interval spanning from 50 cm to 1200 cm. Correlation between the two variables was moderate ($r = 0.51$), and was further improved ($r = 0.68$) after transforming the pCO_2 values into CO_2 concentration via Henry's law. When only considering a partial study period from June to October, the relationship between the variables more closely represented exponential decay, and the best fits were obtained from shorter depth intervals. The noticeable inter-annual variation in the relationship between N and pCO_2 reduced the overall goodness of fit. The largest differences between the predicted and measured values of pCO_2 occurred during weak stratification.

If compared to results obtained in lake Valkea-Kotinen by Huotari et al. (2009, 2011), the relationship between N and pCO_2 in Kuivajärvi isn't as strong and straightforward. The difference in completeness of spring turnovers seems to be an important factor in causing the disparities between the lakes, but various other lake characteristics (e.g size and shape, bathymetry, clarity, catchment area) probably also play a role.

Proxy and measurement based BLM CO_2 fluxes correlated moderately with each other ($r = 0.62$). Comparison between the fluxes revealed that the largest differences between them occurred in May, as the proxy tended to underestimate

pCO_2 values during large spring peaks. On the contrary pCO_2 in June and July was slightly overestimated on average, whereas predictions for the autumn peak could go either way. The comparison to EC flux revealed a large disparity between the two methods. However, such disparities have also been recorded earlier at Kuivajärvi (Erkkilä et al., 2018; Heiskanen et al., 2014; Mammarella et al., 2015), and are related to the parametrisation of k used in BLM.

More studies on the topic in boreal lakes of different characteristics could prove useful. However, it should be noted that as such large inter-annual variation in the relationship between N and surface water pCO_2 was revealed in Kuivajärvi, the measurements done only during a single open water season could easily be misinterpreted.

6. Acknowledgements

I would like to express my gratitude to my supervisor docent Ivan Mammarella for his advice, support and patience during the writing of my thesis, which took considerably longer than originally planned. I also wish to thank professor Petteri Uotila and docent Anne Ojala for their valuable feedback as the reviewers of my thesis.

Bibliography

Åberg, J., Jansson, M., and Jonsson, A. (2010). Importance of water temperature and thermal stratification dynamics for temporal variation of surface water CO2 in a boreal lake. *Journal of Geophysical Research: Biogeosciences*, 115(G02024).

Arst, H., Erm, A., Herlevi, A., Kutser, T., Leppäranta, M., Reinart, A., and Virta, J. (2008). Optical properties of boreal lake waters in finland and estonia. *Boreal Environment Research*, 13:133–158.

Aufdenkampe, A. K., Mayorga, E., Raymond, P. A., Melack, J. M., Doney, S. C., Alin, S. R., Aalto, R. E., and Yoo, K. (2011). Riverine coupling of biogeochemical cycles between land, oceans, and atmosphere. *Frontiers in Ecology and the Environment*, 9(1):53–60.

Bade, D. L. (2010). Gas exchange at the air-water interface. In Likens, G. E., editor, *Biogeochemistry of inland waters : a derivative of Encyclopedia of inland waters*, pages 28–36. Elsevier/Academic Press.

Battin, T. J., Luyssaert, S., Kaplan, L. A., Aufdenkampe, A. K., Richter, A., and Tranvik, L. J. (2009). The boundless carbon cycle. *Nature Geoscience*, 2(9):598–600.

Cole, J. J. and Caraco, N. F. (1998). Atmospheric exchange of carbon dioxide in a low-wind oligotrophic lake measured by the addition of SF6. *Limnology and Oceanography*, 43(4):647–656.

Cole, J. J., Caraco, N. F., Kling, G. W., and Kratz, T. K. (1994). Carbon dioxide supersaturation in the surface waters of lakes. *Science*, 265(5178):1568–1570.

Cole, J. J. and Prairie, Y. T. (2010a). Carbon, unifying currency. In Likens, G. E., editor, *Biogeochemistry of inland waters : a derivative of Encyclopedia of inland waters*, pages 453–456. Elsevier/Academic Press.

Cole, J. J. and Prairie, Y. T. (2010b). Dissolved CO2. In Likens, G. E., editor, *Biogeochemistry of inland waters : a derivative of Encyclopedia of inland waters*, pages 343–347. Elsevier/Academic Press.

Cole, J. J., Prairie, Y. T., Caraco, N. F., McDowell, W. H., Tranvik, L. J., Striegl, R. G., Duarte, C. M., Kortelainen, P., Downing, J. A., Middelburg, J. J., and Melack, J. (2007). Plumbing the global carbon cycle: Integrating inland waters into the terrestrial carbon budget. *Ecosystems*, 10(1):172–185.

Erkkilä, K.-M., Ojala, A., Bastviken, D., Biermann, T., Heiskanen, J. J., Lindroth, A., Peltola, O., Rantakari, M., Vesala, T., and Mammarella, I. (2018). Methane and carbon dioxide fluxes over a lake: comparison between eddy covariance, floating chambers and boundary layer method. *Biogeosciences*, 15:429–445.

Foken, T., Leuning, R., Oncley, S. R., Mauder, M., and Aubinet, M. (2012). Corrections and data quality control. In Aubinet, M., Vesala, T., and Papale, D., editors, *Eddy Covariance*, pages 85–131. Springer Netherlands.

Hari, P. and Kulmala, M. (2005). Station for measuring ecosystem-atmosphere relations (smear ii). *Boreal Environment Research*, 10(5):315–322.

Hari, P., Pumpanen, J., Huotari, J., Kolari, P., Grace, J., Vesala, T., and Ojala, A. (2008). High-frequency measurements of productivity of planktonic algae using rugged nondispersive infrared carbon dioxide probes. *Limnology and Oceanography: Methods*, 6(8):347–354.

Heiskanen, J. J., Mammarella, I., Haapanala, S., Pumpanen, J., Vesala, T., MacIntyre, S., and Ojala, A. (2014). Effects of cooling and internal wave motions on gas transfer coefficients in a boreal lake. *Tellus B: Chemical and Physical Meteorology*, 66(1):22827.

Heiskanen, J. J., Mammarella, I., Ojala, A., Stepanenko, V., Erkkilä, K.-M., Miettinen, H., Sandström, H., Eugster, W., Leppäranta, M., Järvinen, H., Vesala, T., and Nordbo, A. (2015). Effects of water clarity on lake stratification and lake-atmosphere heat exchange. *Journal of Geophysical Research: Atmospheres*, 120(15):7412–7428.

Huotari, J., Ojala, A., Peltomaa, E., Nordbo, A., Launiainen, S., Pumpanen, J., Rasilo, T., Hari, P., and Vesala, T. (2011). Long-term direct CO2 flux measurements over a boreal lake: Five years of eddy covariance data. *Geophysical Research Letters*, 38(18):n/a–n/a.

Huotari, J., Ojala, A., Peltomaa, E., Pumpanen, J., Hari, P., and Vesala, T. (2009). Temporal variations in surface water CO2 concentrations in a boral humic lake base on high-frequency measurements. *Boreal Environment Research*, 14:48–60.

Jähne, B., Heinz, G., and Dietrich, W. (1987). Measurement of the diffusion coefficients of sparingly soluble gases in water. *Journal of Geophysical Research*, 92(C10):10767.

Karlsson, J., Giesler, R., Persson, J., and Lundin, E. (2013). High emission of carbon dioxide and methane during ice thaw in high latitude lakes. *Geophysical Research Letters*, 40(6):1123–1127.

Korhonen, J. (2005). *Suomen vesistojen jaaolot*. Suomen ymparistokeskus, Helsinki.

Kortelainen, P., Rantakari, M., Huttunen, J. T., Mattsson, T., Alm, J., Juutinen, S., Larmola, T., Silvola, J., and Martikainen, P. J. (2006). Sediment respiration and lake trophic state are important predictors of large CO2 evasion from small boreal lakes. *Global Change Biology*, 12(8):1554–1567.

Leppäranta, M., Virta, J., and Huttula, T. (2017). *Hydrologian perusteet*. Helsingin yliopisto, Fysiikan laitos 2017, Unigrafia.

MacIntyre, S., Wanninkhof, R., and Chanton, J. P. (1995). *Biogenic trace gases: measuring emissions from soil and water*, chapter Trace gas exchange across the air-water interface in freshwater and coastal marine environments, pages 52–97. Blackwell Science Ltd, 1995.

Mammarella, I., Gavrylenko, G., Zdorovennova, G., Ojala, A., Erkkilä, K.-M., Zdorovennov, R., Stepanyuk, O., Palshin, N., Terzhevik, A., Vesala, T., and Heiskanen, J. (2018). Effects of similar weather patterns on the thermal stratification, mixing regimes and hypolimnetic oxygen depletion in two boreal lakes with different water transparency. *Boreal Environment Research*, 23:237–247.

Mammarella, I., Nordbo, A., Üllar Rannik, Haapanala, S., Levula, J., Laakso, H., Ojala, A., Peltola, O., Heiskanen, J., Pumpanen, J., and Vesala, T. (2015). Carbon dioxide and energy fluxes over a small boreal lake in Southern Finland. *Journal of Geophysical Research: Biogeosciences*, 120(7):1296–1314.

Miettinen, H., Pumpanen, J., Heiskanen, J., Aaltonen, H., Mammarella, I., Ojala, A., Levula, J., and Rantakari, M. (2015). Towards a more comprehensive understanding of lacustrine greenhouse gas dynamics — two-year measurements of

concentrations and fluxes of CO2, CH4 and N2O in a typical boreal lake surrounded by managed forests. *Boreal Environment Research*, 20:75–89.

Miettinen, H., Pumpanen, J., Rantakari, M., and Ojala, A. (2020). Carbon dynamics in a boreal land-stream-lake continuum during the spring freshet of two hydrologically contrasting years. *Biogeochemistry*, 148(1):91–109.

Munger, J. W., Loescher, H. W., and Luo, H. (2012). Measurement, tower, and site design considerations. In Aubinet, M., Vesala, T., and Papale, D., editors, *Eddy Covariance*, pages 21–58. Springer Netherlands.

Pirinen, P. (2012). *Tilastoja Suomen ilmastosta 1981-2010*. Ilmatieteen Laitos, Helsinki.

Rantakari, M. and Kortelainen, P. (2005). Interannual variation and climatic regulation of the CO2 emission from large boreal lakes. *Global Change Biology*, 11(8):1368–1380.

Raymond, P. A., Hartmann, J., Lauerwald, R., Sobek, S., McDonald, C., Hoover, M., Butman, D., Striegl, R., Mayorga, E., Humborg, C., Kortelainen, P., Dürr, H., Meybeck, M., Ciais, P., and Guth, P. (2013). Global carbon dioxide emissions from inland waters. *Nature*, 503(7476):355–359.

Rebmann, C., Kolle, O., Heinesch, B., Queck, R., Ibrom, A., and Aubinet, M. (2012). Data acquisition and flux calculations. In Aubinet, M., Vesala, T., and Papale, D., editors, *Eddy Covariance*, pages 59–83. Springer Netherlands.

Tranvik, L. J., Downing, J. A., Cotner, J. B., Loiselle, S. A., Striegl, R. G., Ballatore, T. J., Dillon, P., Finlay, K., Fortino, K., Knoll, L. B., Kortelainen, P. L., Kutser, T., Larsen, S., Laurion, I., Leech, D. M., McCallister, S. L., McKnight, D. M., Melack, J. M., Overholt, E., Porter, J. A., Prairie, Y., Renwick, W. H., Roland, F., Sherman, B. S., Schindler, D. W., Sobek, S., Tremblay, A., Vanni, M. J., Verschoor, A. M., von Wachenfeldt, E., and Weyhenmeyer, G. A. (2009). Lakes and reservoirs as regulators of carbon cycling and climate. *Limnology and Oceanography*, 54(6, part 2):2298–2314.

Vesala, T., Eugster, W., and Ojala, A. (2012). Eddy covariance measurements over lakes. In Aubinet, M., Vesala, T., and Papale, D., editors, *Eddy Covariance*, pages 365–376. Springer Netherlands.

Wanninkhof, R. (2014). Relationship between wind speed and gas exchange over the ocean revisited. *Limnology and Oceanography: Methods*, 12(6):351–362.

Weyhenmeyer, G. A., Kortelainen, P., Sobek, S., Müller, R., and Rantakari, M. (2012). Carbon dioxide in boreal surface waters: A comparison of lakes and streams. *Ecosystems*, 15(8):1295–1307.